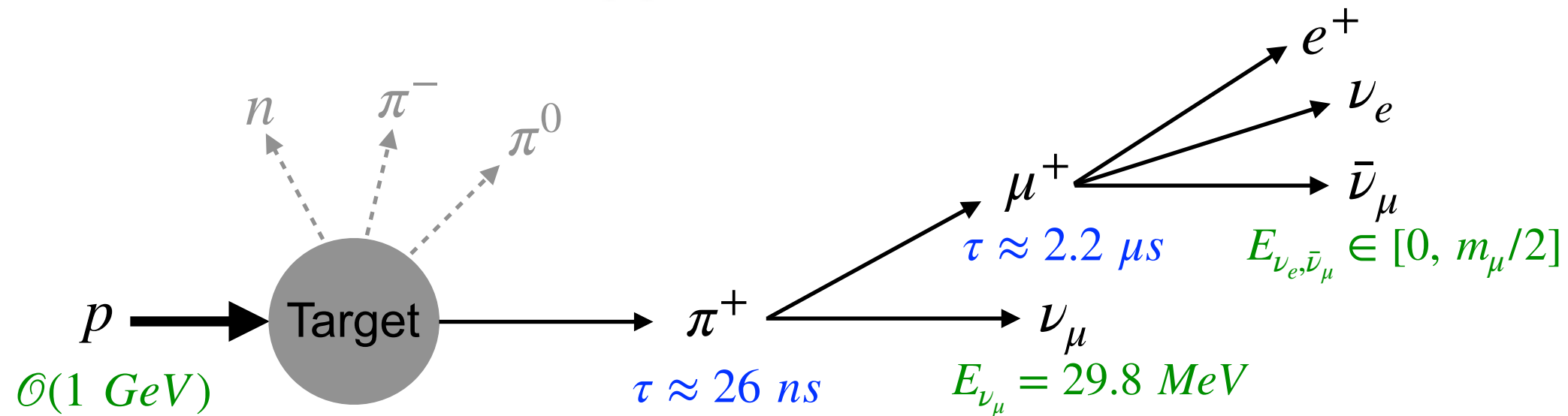


Synergy between Nuclear Physics in CEvNS and Long-baseline Neutrino Experiments

Vishvas Pandey



Stopped-Pion Sources and CEvNS



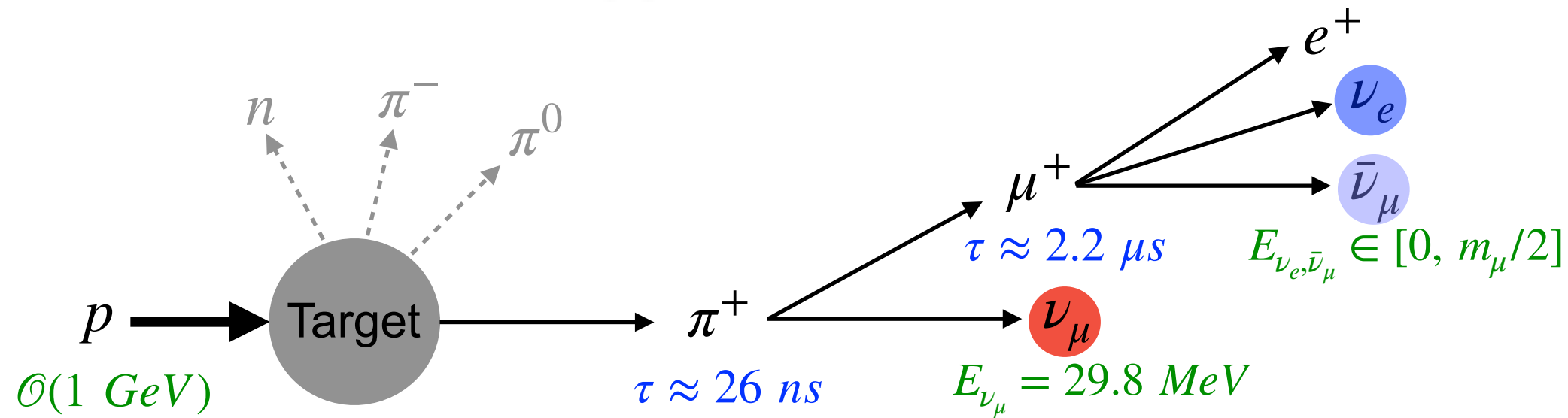
- **Proton energy:**

- Sufficient energy ($\sim 1 \text{ GeV}$) to produce pions
[SNS at ORNL, Lujan at LANL]
- Higher energies lead to heavier mesons: kaons ($> 3 \text{ GeV}$), eta
[JPARC-MLF]

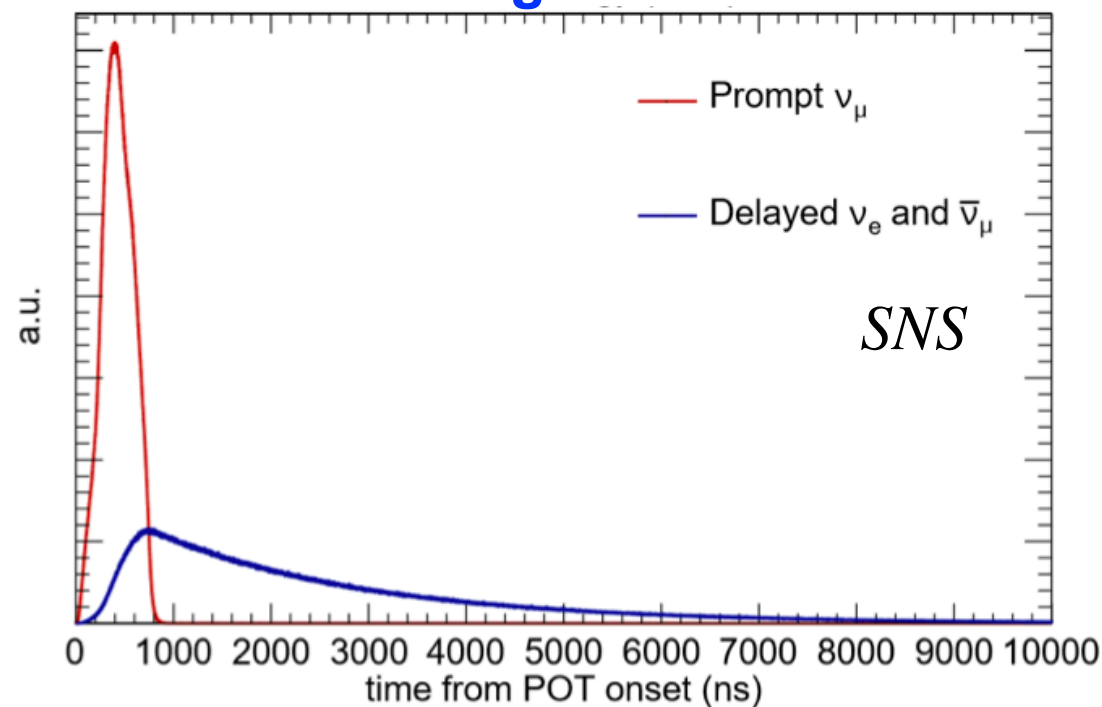
- **Target:**

- Heavier targets at spallation sources massively produce neutrons (primary motive)
[Hg at SNS at ORNL and JPARC-MLF, W at Lujan at LANL]
- For a dedicated hep facility lighter targets would be preferred (low neutrons from beam)
- Neutrons mimic the same signature as CEvNS

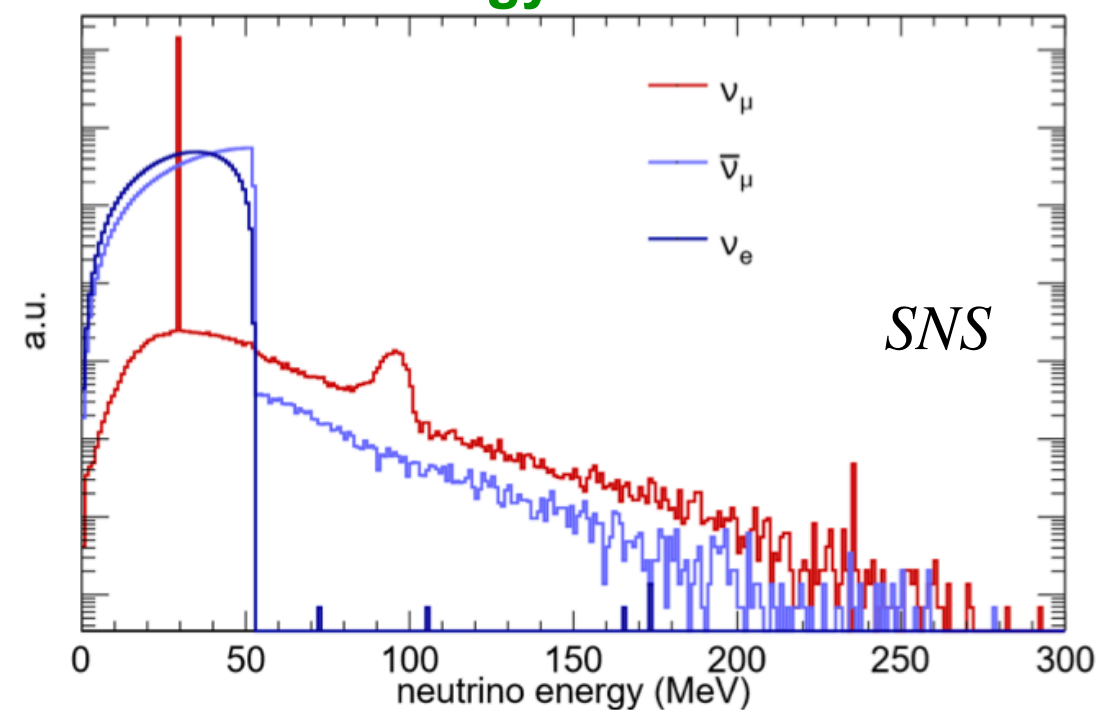
Stopped-Pion Sources and CEvNS



Timing Profile



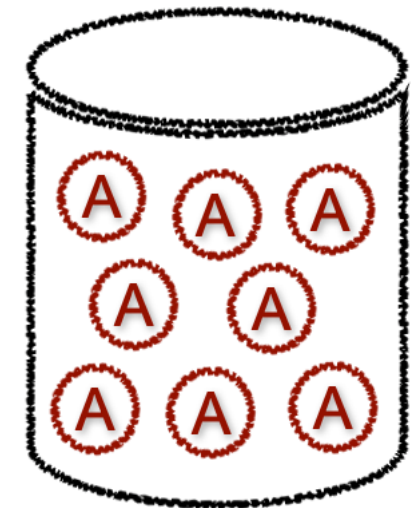
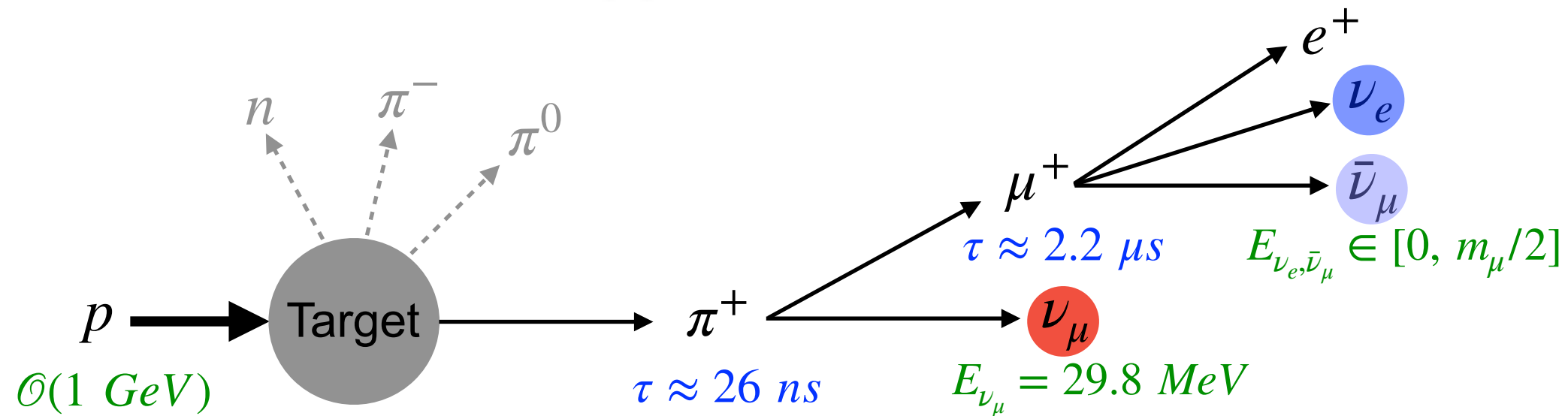
Energy Profile



D. Akimov et al. [COHERENT], Science 357, 6356, 1123–1126 (2017)

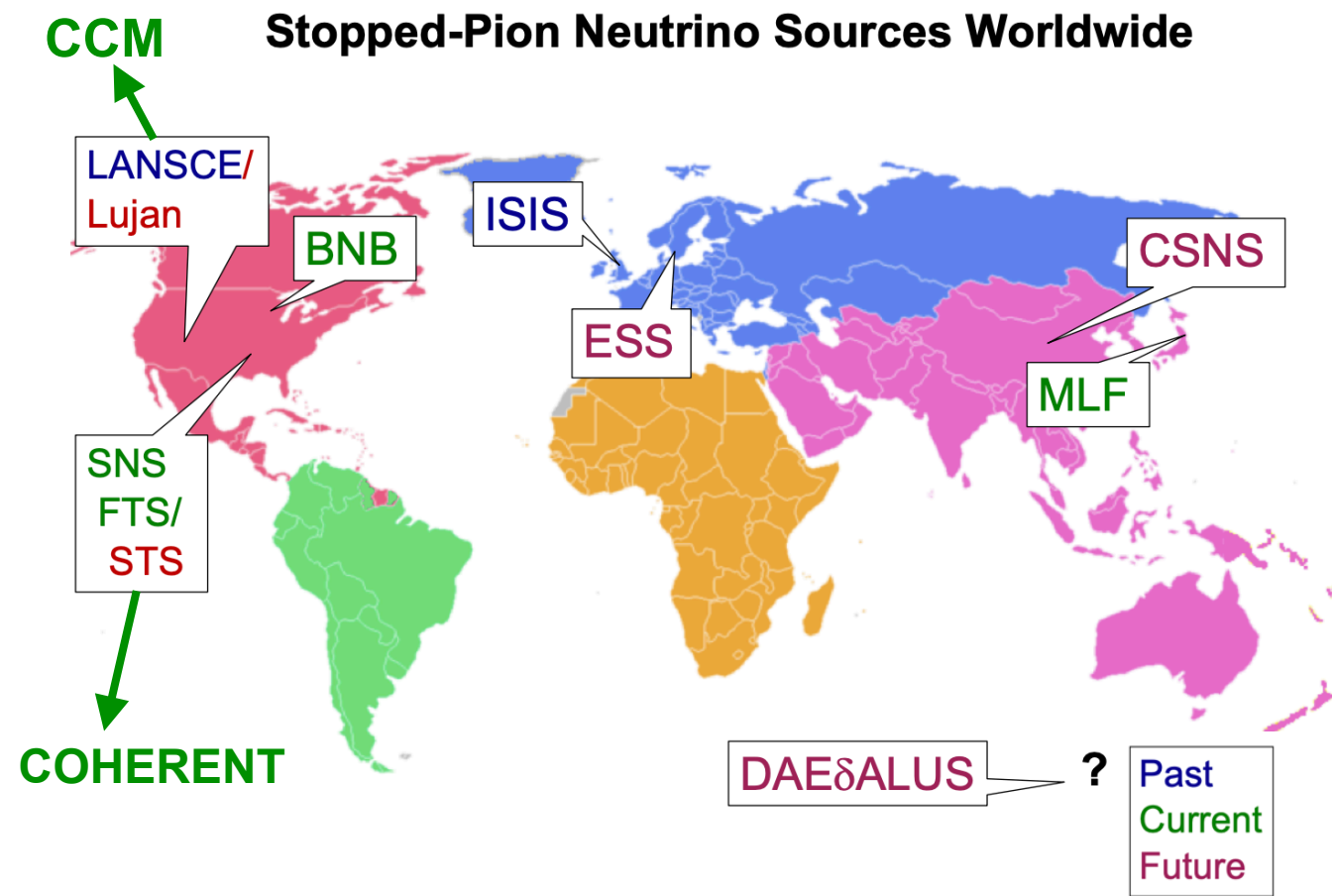
- Proton pulse duration and time between different pulses are key factors
 - For beam spills $< \mu^+$ lifetime: can separate piDAR and muDAR neutrinos
 - For beam spills $< \pi^+$ lifetime: can separate light dark matter production (from π^0 , η) from neutrino production

Stopped-Pion Sources and CEvNS

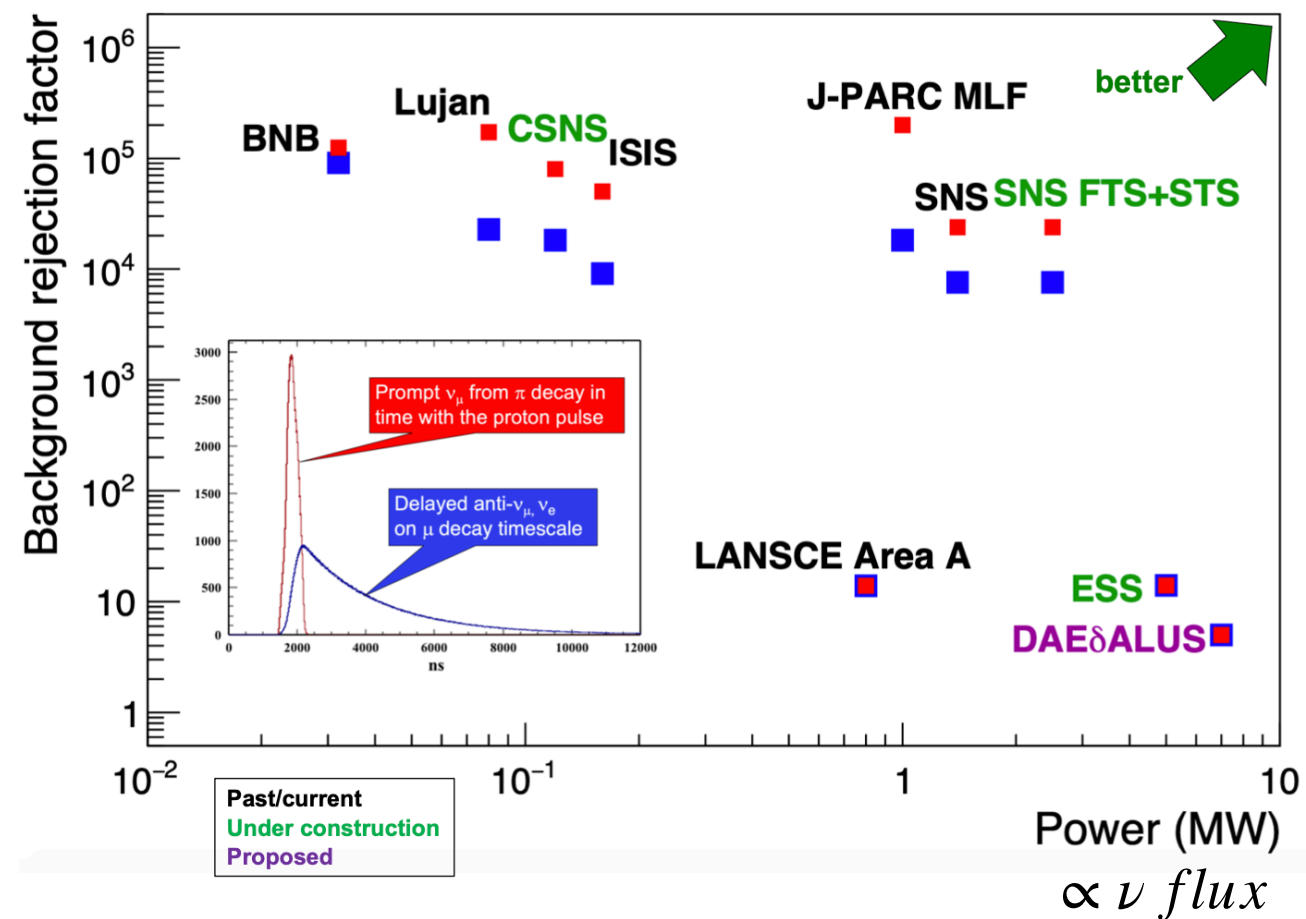


Low threshold (~keV) detector

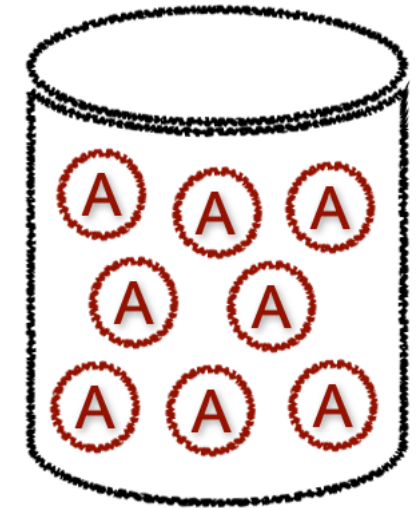
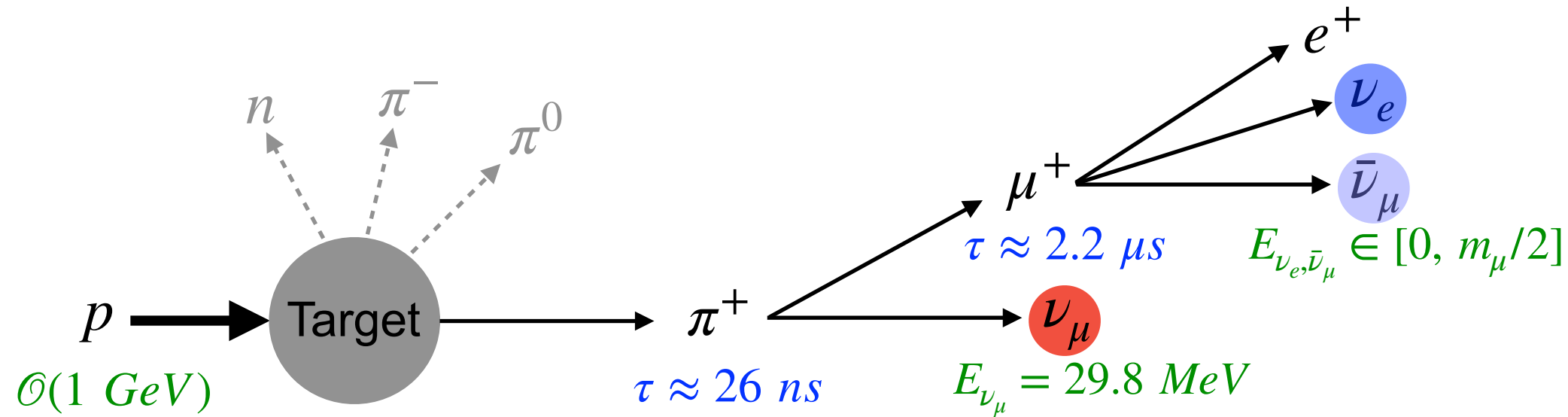
Stopped-Pion Neutrino Sources Worldwide



Flavor separation with beam timing can be helpful!



Stopped-Pion Sources and CEvNS

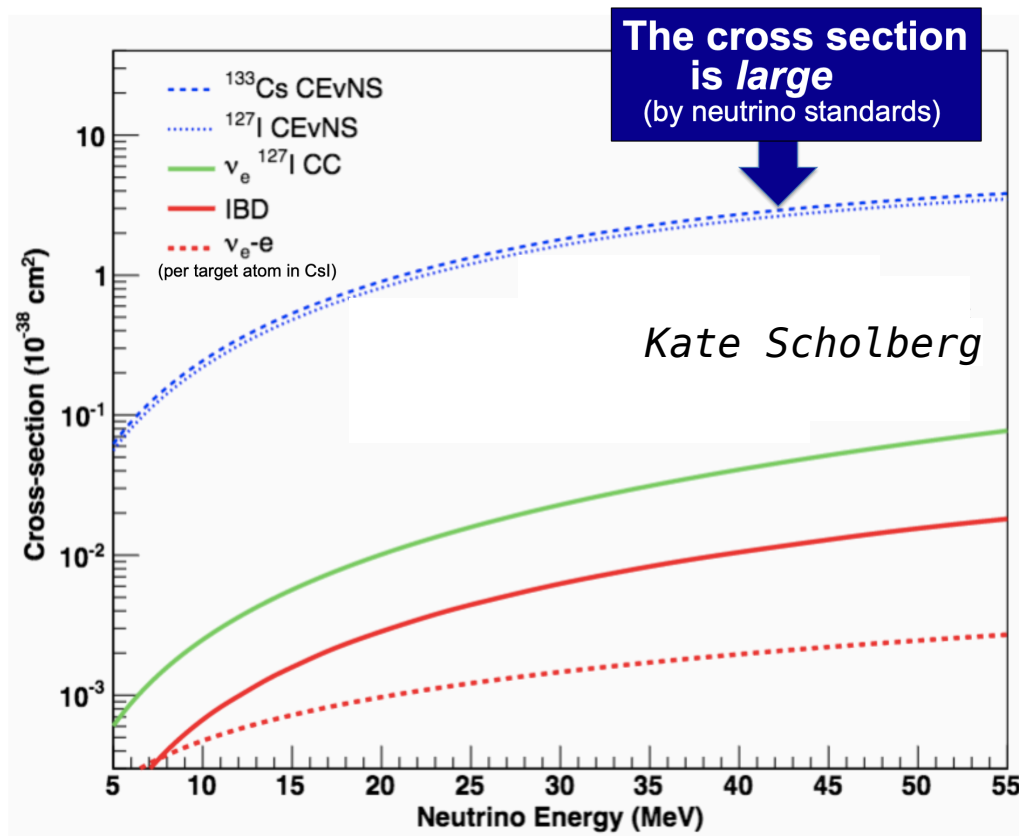


Low threshold (\sim keV) detector

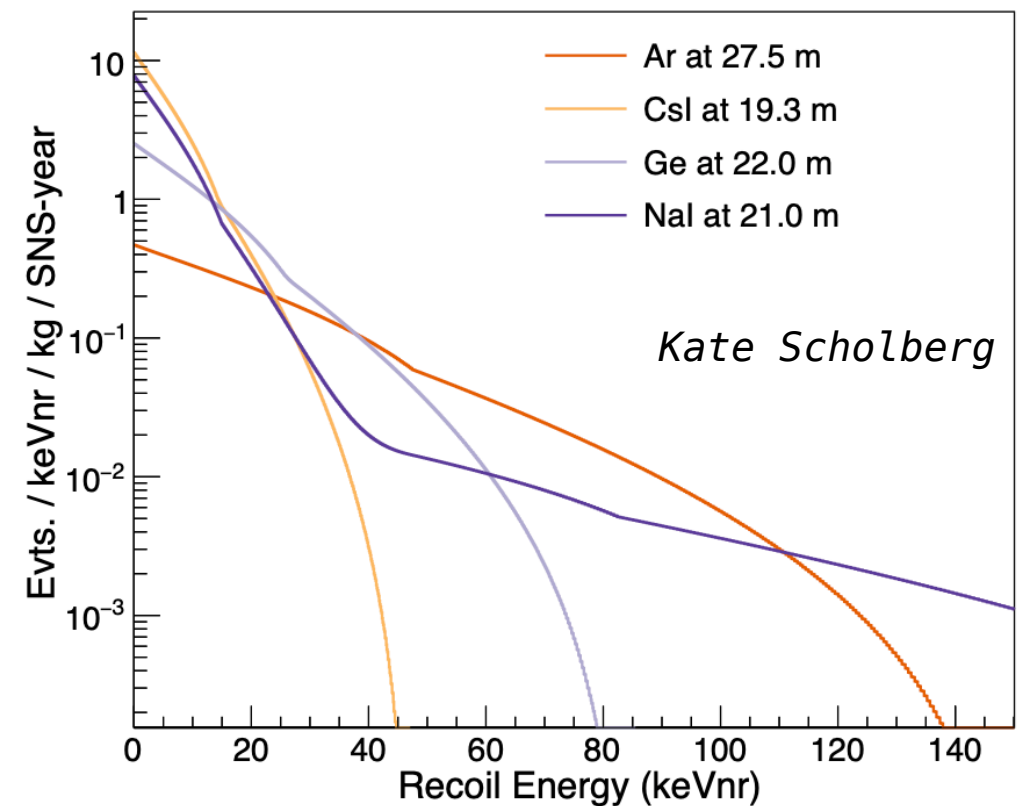
Coherent elastic neutrino-nucleus scattering (CEvNS):

- Large cross section but tiny recoil
- Only experimental signature: keV energy deposited by nuclear recoil in the target material
- Recent R&D in dark matter and $0\nu\beta\beta$ detector technologies helped overcoming long standing (> 40 years) hurdle

Large cross section



Tiny nuclear recoil

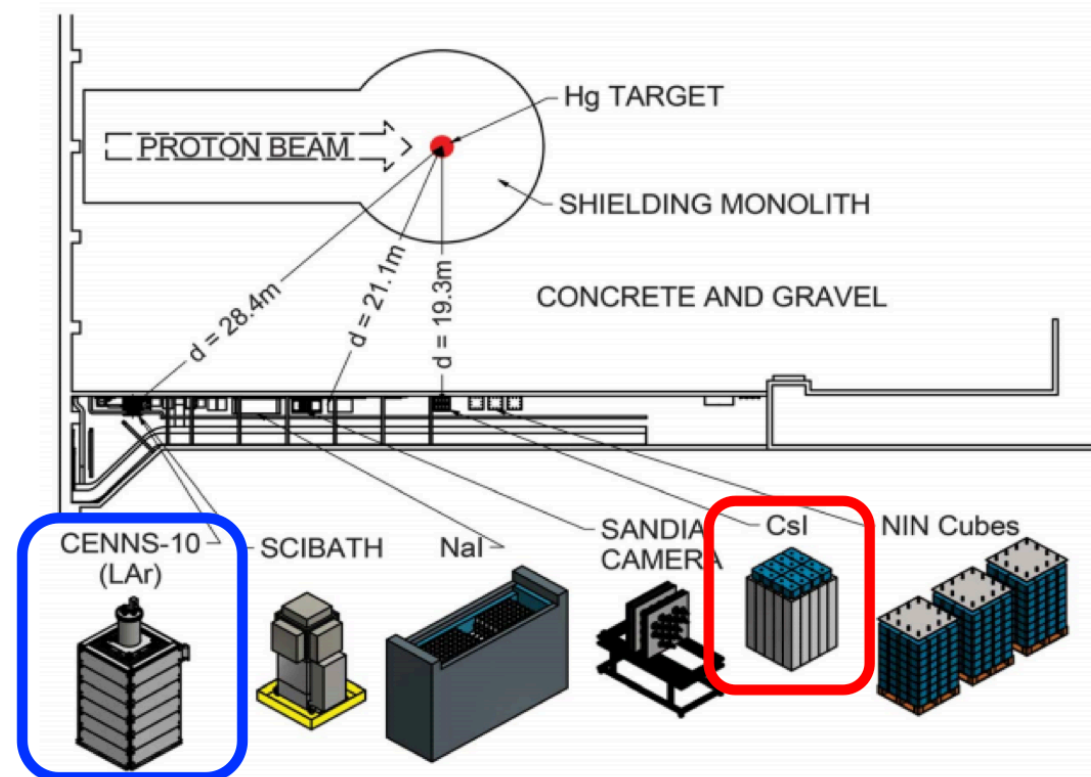
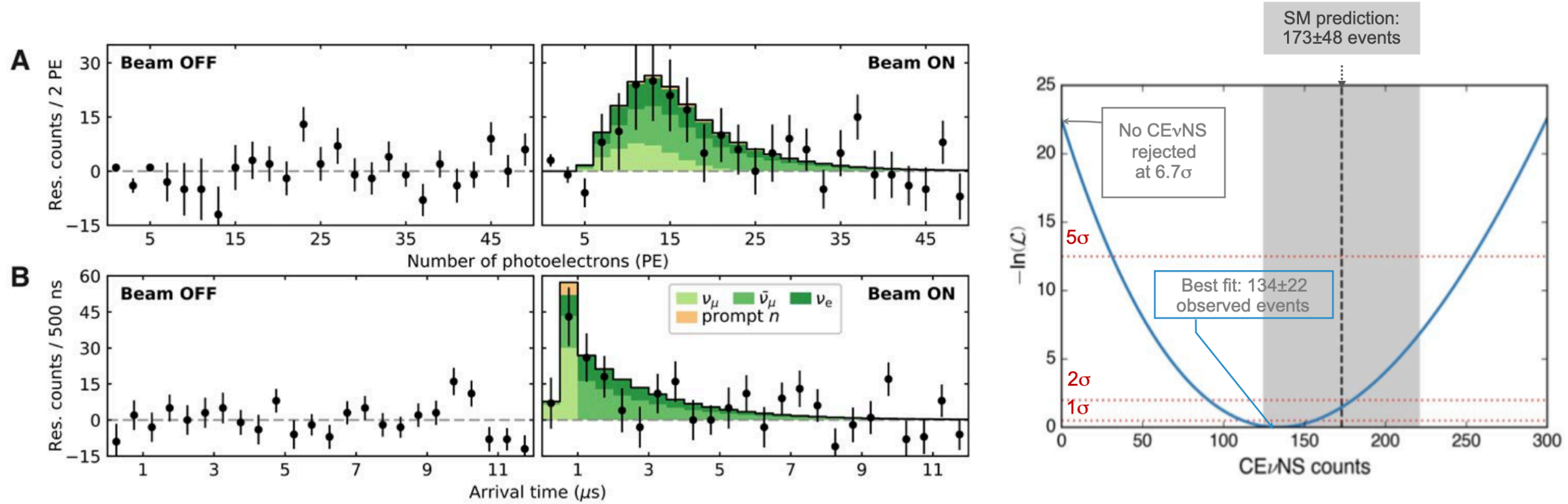


Observing CEvNS

COHERENT Collaboration at SNS at ORNL

14 kg Csi detector

D. Akimov et al. [COHERENT], Science 357, 6356, 1123–1126 (2017)

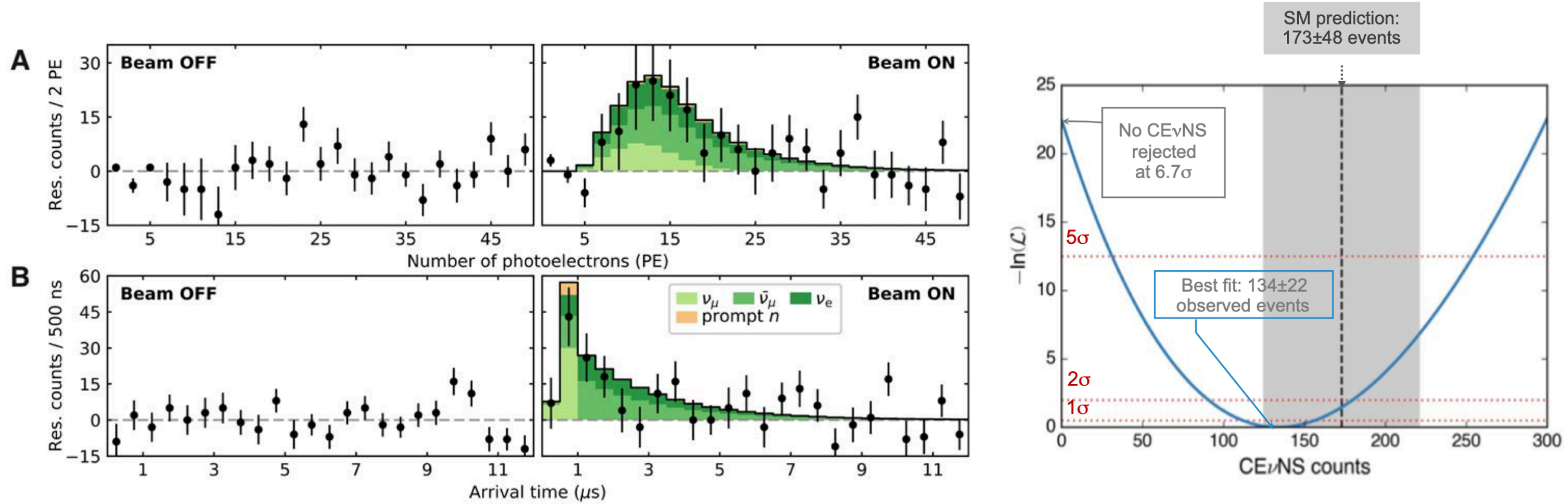


Observing CEvNS

COHERENT Collaboration at SNS at ORNL

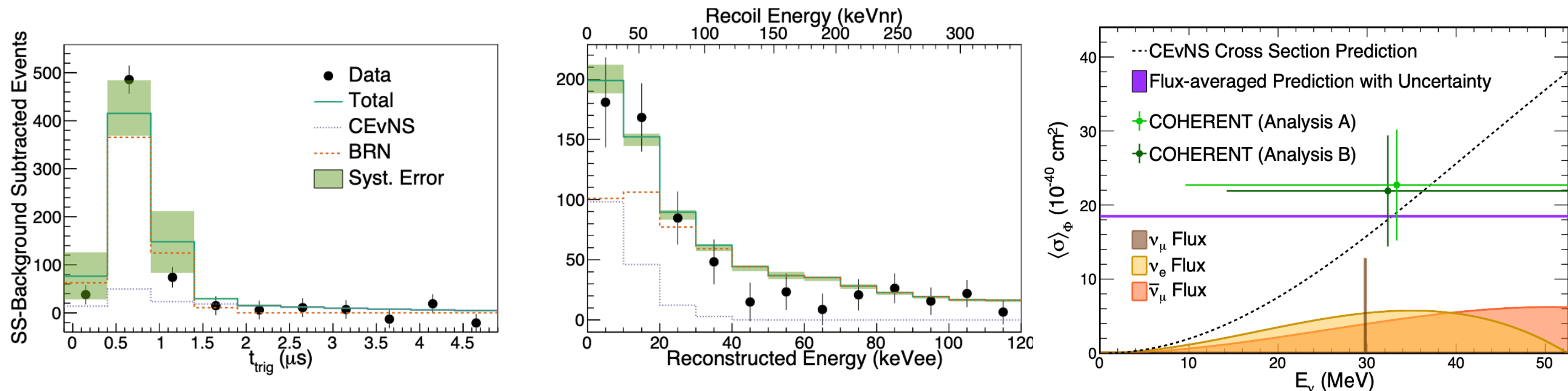
14 kg CSI detector

D. Akimov et al. [COHERENT], Science 357, 6356, 1123–1126 (2017)



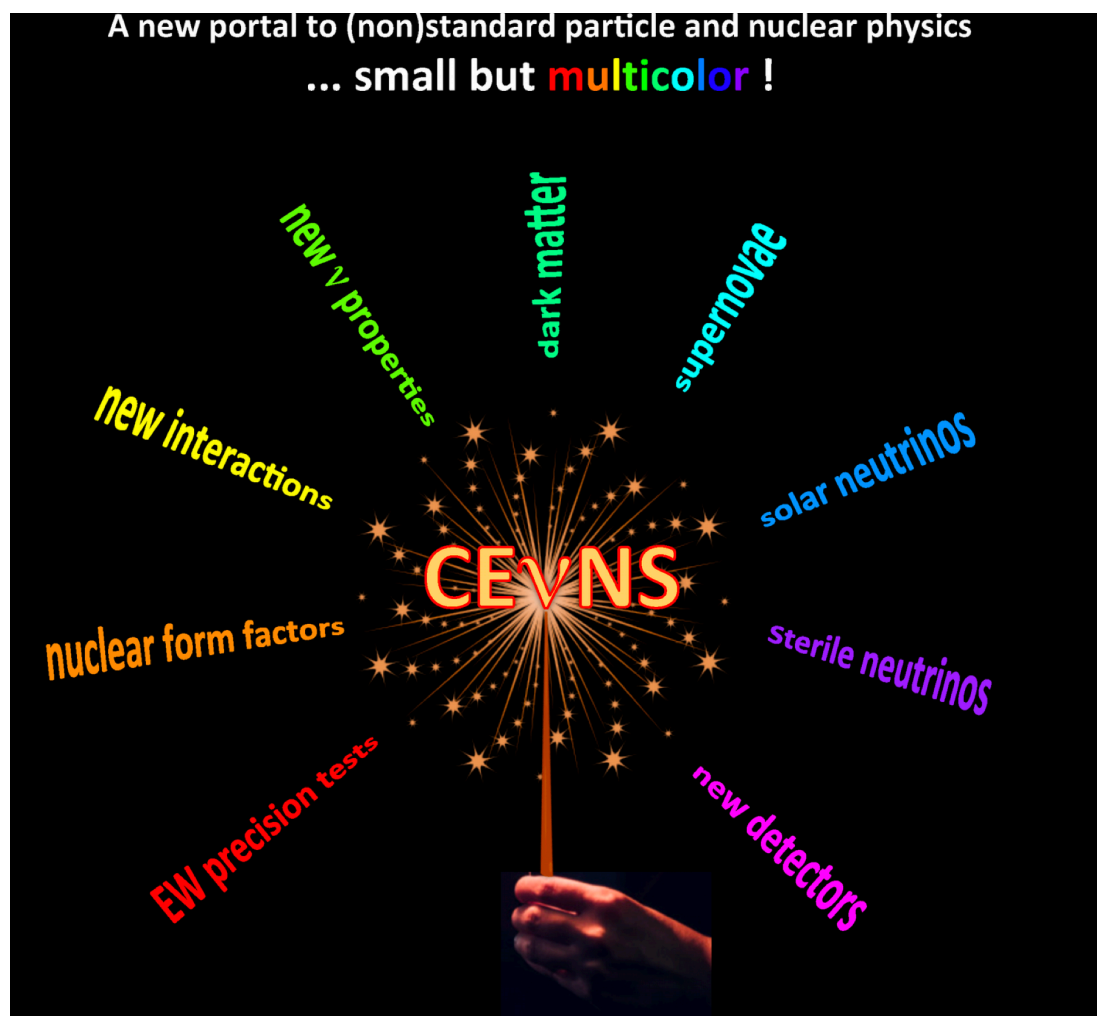
24 kg LAr (CENNS-10) detector

D. Akimov et al. [COHERENT], arXiv:2003.10630 [nucl-ex]



CEvNS: A New Portal to Standard and Non-Standard Physics

- New physics may be weakly interacting and hiding at low energies
- Any deviation from the SM expectation → new physics
- SM expectation of CEvNS cross section have to be know at a precision that allows resolving degeneracies in the standard and non-standard physics observables

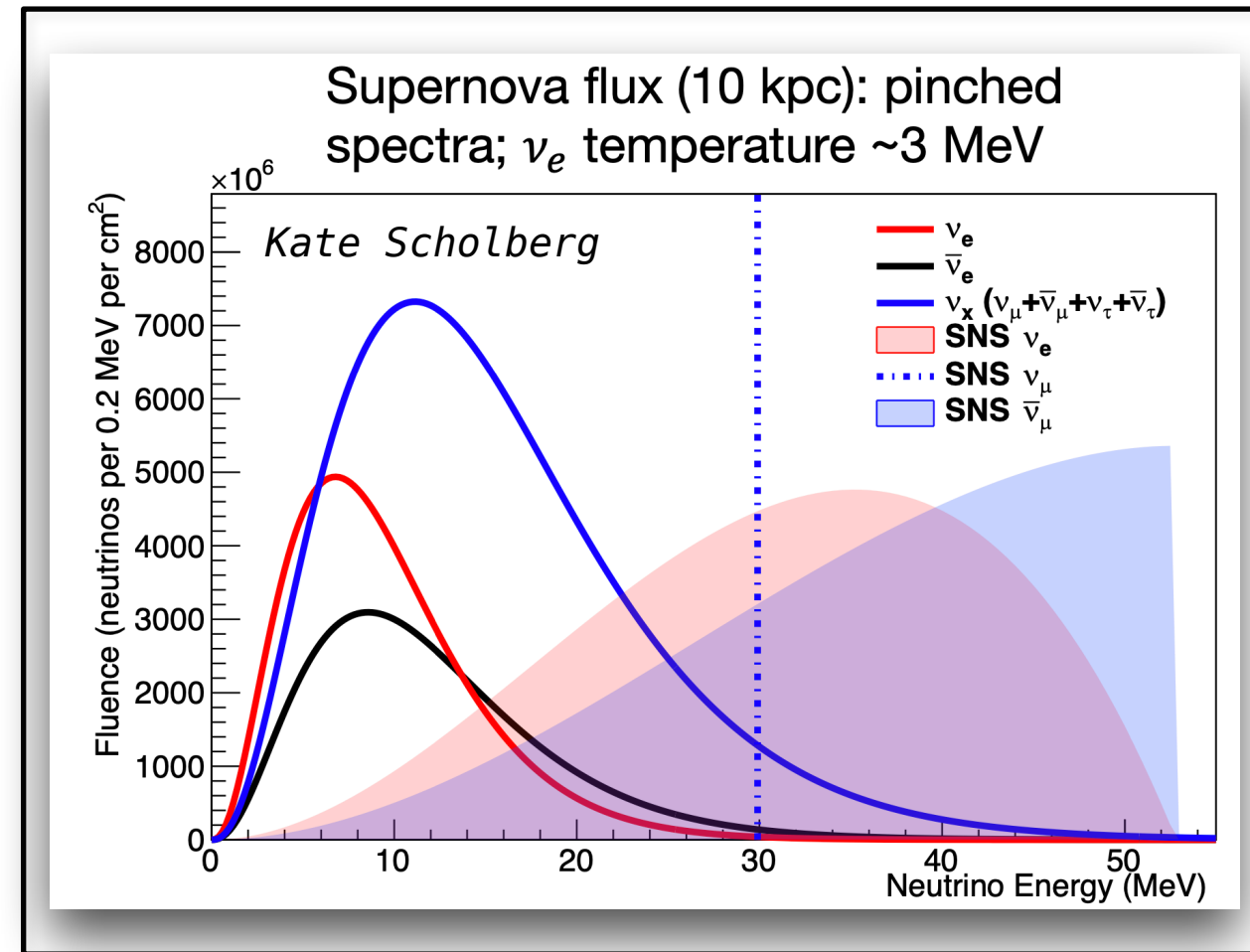
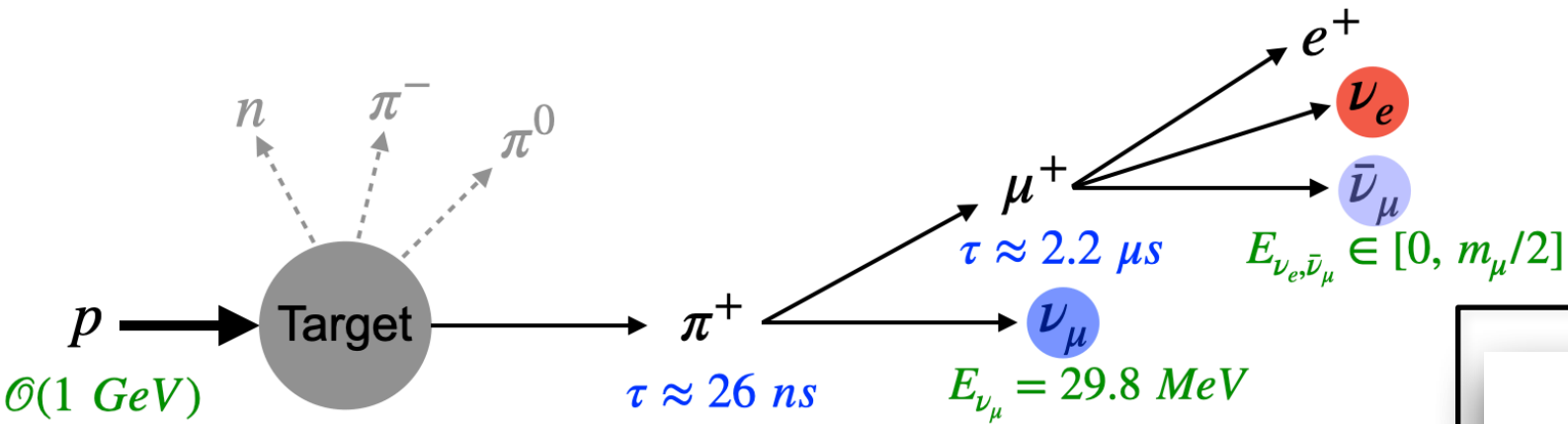


Eligio Lisi, NuINT 2018

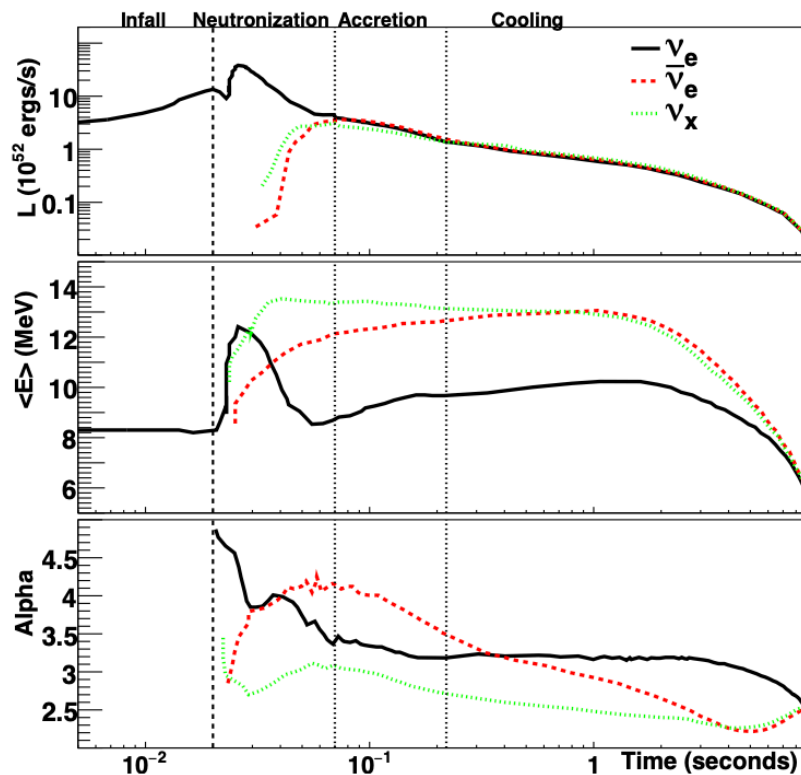


Matteo Cadettu, Magnificent CEvNS 2020

Stopped-Pion Sources and Supernova Neutrinos



◆ Neutrinos from stopped-pion sources and from supernova carry similar energies.

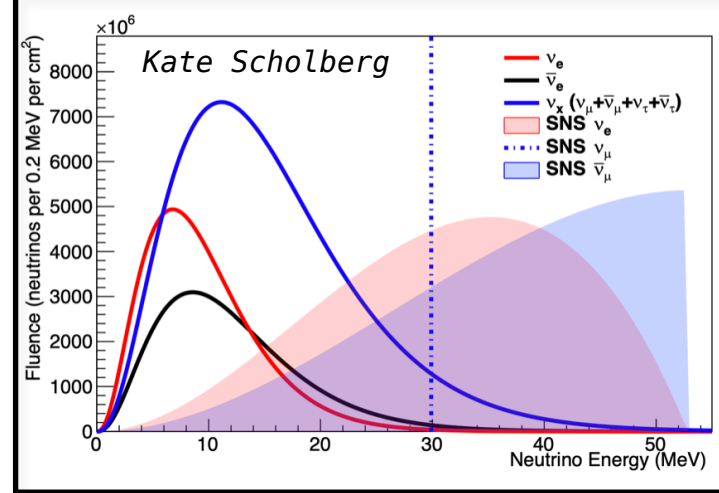
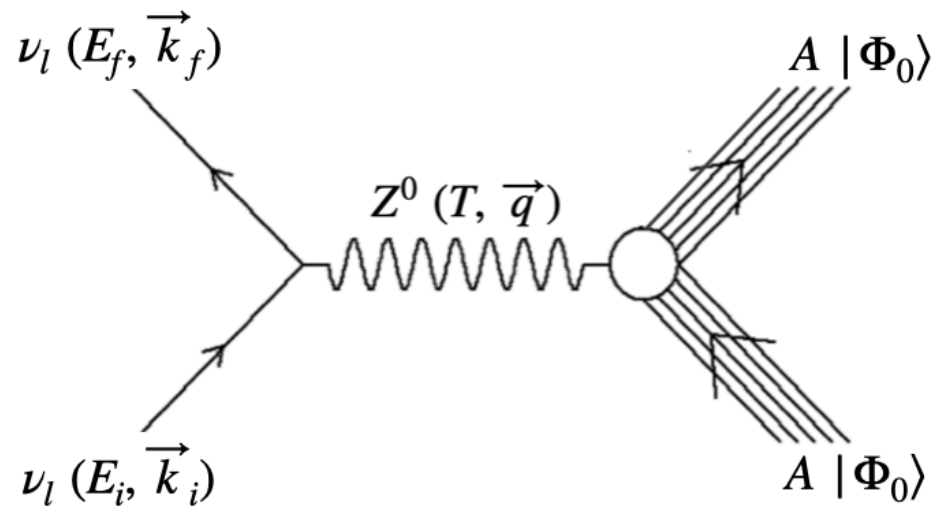


Neutrino signal from the core-collapse supernova starts with a short, sharp “neutronization” (or “breakout”) burst primarily composed of ν_e from $e^- + p \rightarrow \nu_e + n$.

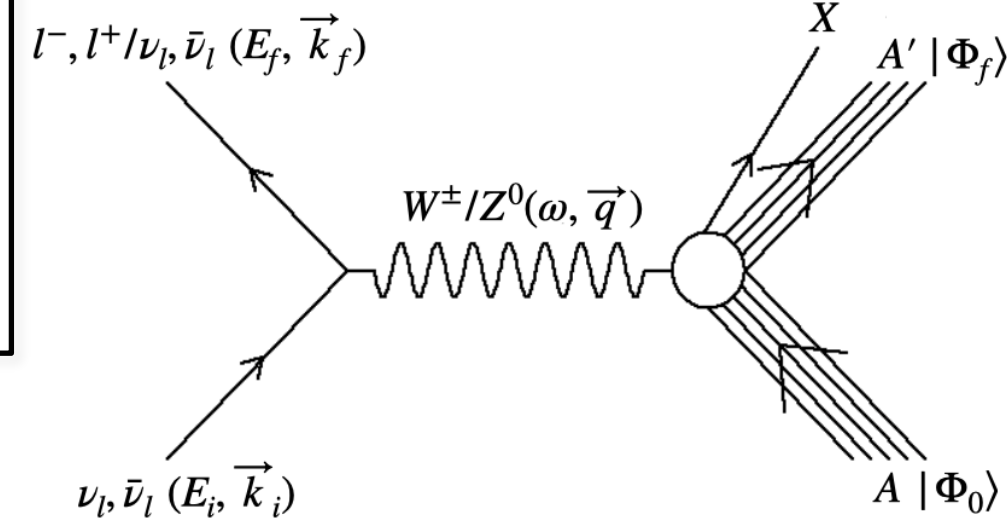
[arXiv:2008.06647 \[hep-ex\] \[DUNE Collaboration\]](https://arxiv.org/abs/2008.06647)

Coherent Elastic and Inelastic Neutrino-Nucleus Scattering

Coherent elastic [CEvNS]



Inelastic CC/NC

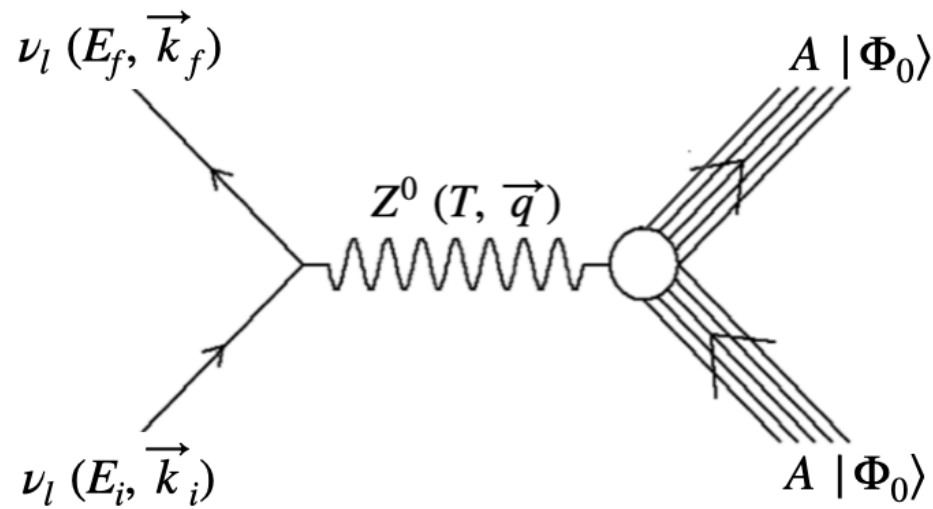


- Tiny recoil energy, large cross section
- Final state nucleus stays in its ground state
- Signal: keV energy nuclear recoil (gammas)

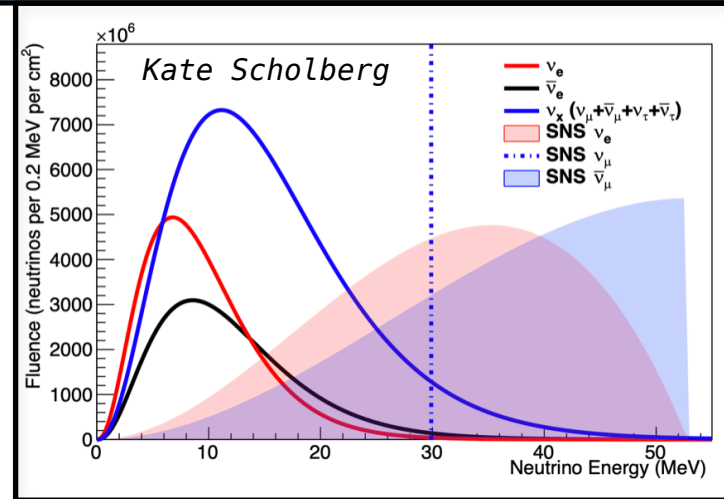
- Small energy transferred to the nucleus
- Nucleus excites to states with well-defined excitation energy, spin and parity (J^π)
- Followed by nuclear de-excitation into gammas, p, n, and nuclear fragmentations.

Coherent Elastic and Inelastic Neutrino-Nucleus Scattering

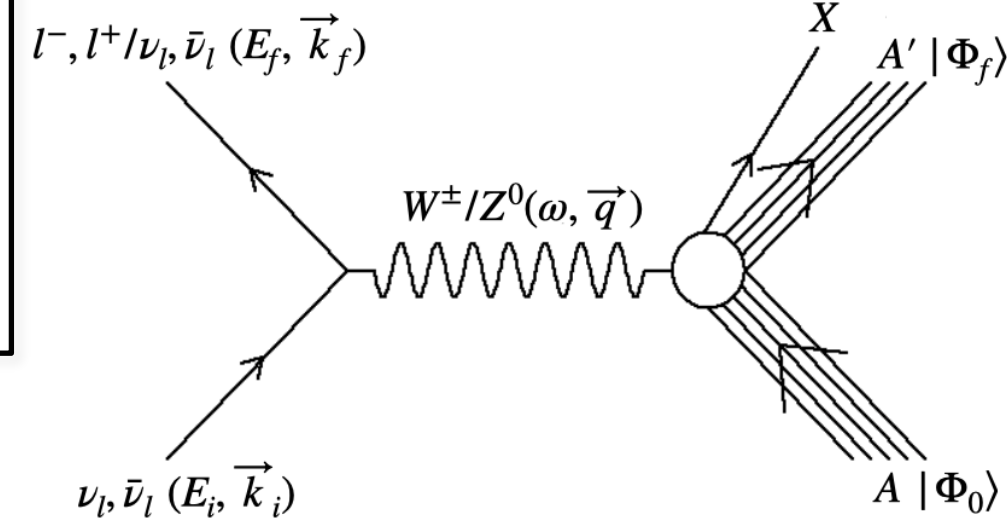
Coherent elastic [CEvNS]



- Tiny recoil energy, large cross section
- Final state nucleus stays in its ground state
- Signal: keV energy nuclear recoil (gammas)



Inelastic CC/NC



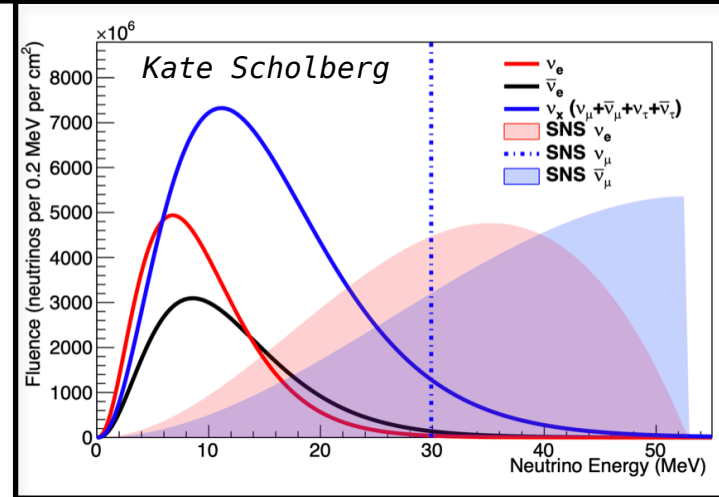
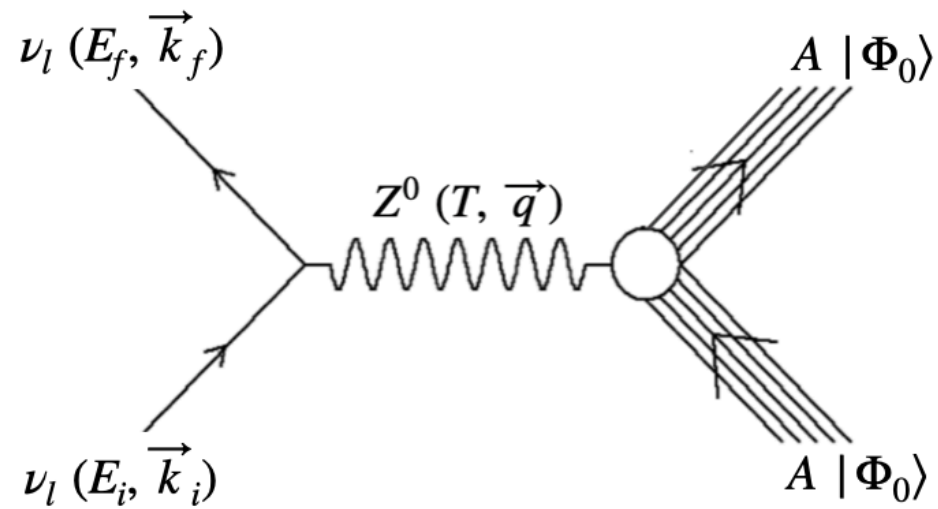
- Small energy transferred to the nucleus
- Nucleus excites to states with well-defined excitation energy, spin and parity (J^π)
- Followed by nuclear de-excitation into gammas, p, n, and nuclear fragmentations.

◆ CEvNS experiments at stopped-pion sources are powerful avenues

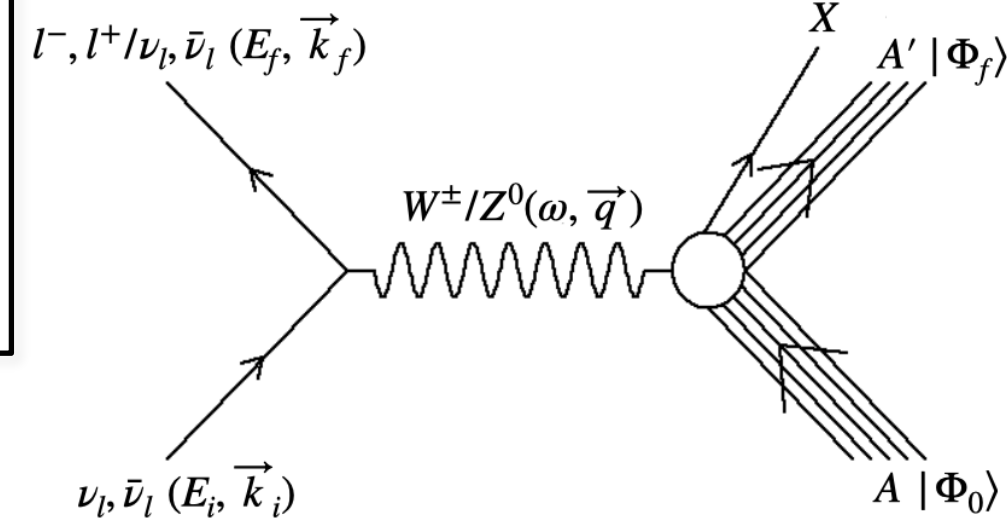
- to constrain poorly known **weak form factors** (at low momentum transfers) and **neutron density distributions** in nuclei. These are vital input in modeling ground states of nuclei.
- to measure poorly known **10s of MeV inelastic CC and NC** cross sections. These measurements will play a vital role in enhancing future long baseline neutrino experiments' capability of detecting **core-collapse supernovae neutrinos**.

Coherent Elastic and Inelastic Neutrino-Nucleus Scattering

Coherent elastic [CEvNS]



Inelastic CC/NC



$$\sum_{fi} |\mathcal{M}|^2 \propto \frac{G_F^2}{2} L_{\mu\nu} W^{\mu\nu}$$

Leptonic Tensor: $L_{\mu\nu} = \sum_{fi} (\mathcal{J}_{l,\mu})^\dagger \mathcal{J}_{l,\nu}$

Hadronic Tensor: $W^{\mu\nu} = \sum_{fi} (\mathcal{J}_n^\mu)^\dagger \mathcal{J}_n^\nu$

Transition Amplitude: $\mathcal{J}_n^\mu = \langle \Phi_0 | \hat{J}_n^\mu(q) | \Phi_0 \rangle$

Transition Amplitude: $\mathcal{J}_n^\mu = \langle \Phi_f | \hat{J}_n^\mu(q) | \Phi_0 \rangle$

Cross Section:

$$d\sigma \propto \frac{G_F^2}{4\pi} Q_W^2 F_W^2(q)$$

Cross Section:

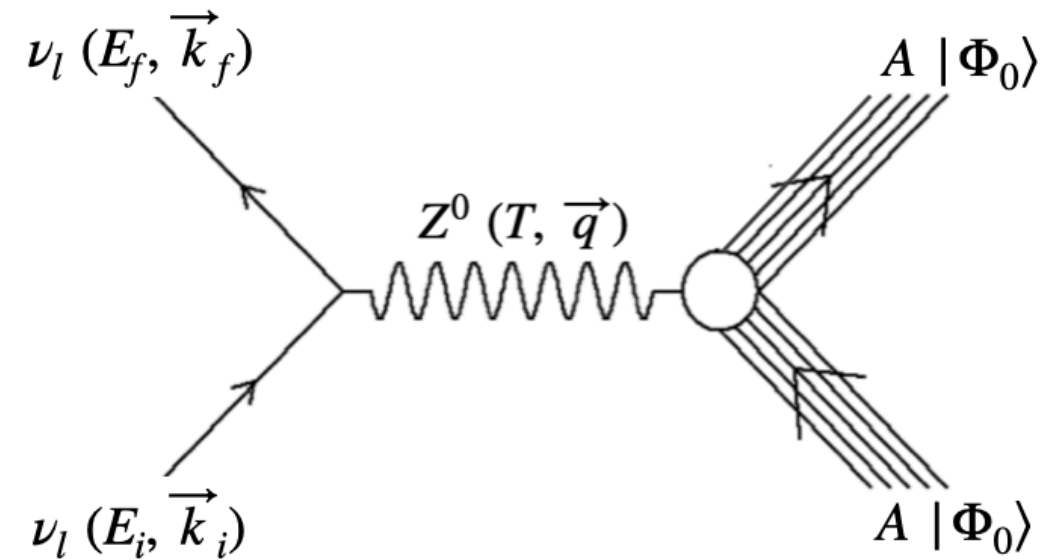
$$d\sigma \propto \frac{G_F^2}{4\pi} \sum_{J^\pi} [v_{CC} W_{CC} + v_{CL} W_{CL} + v_{LL} W_{LL} + v_T W_T \pm v_{T'} W_{T'}]$$

CEvNS Cross Section and Form Factors

■ Cross section:

$$\frac{d\sigma}{dT} = \frac{G_F^2}{\pi} M_A \left[1 - \frac{T}{E_i} - \frac{M_A T}{2E_i^2} \right] \frac{Q_W^2}{4} F_W^2(q)$$

$$\frac{d\sigma}{d\cos\theta_f} = \frac{G_F^2}{2\pi} E_i^2 (1 + \cos\theta_f) \frac{Q_W^2}{4} F_W^2(q)$$



$$T \in \left[0, \frac{2E_i^2}{(M_A + 2E_i)} \right]$$

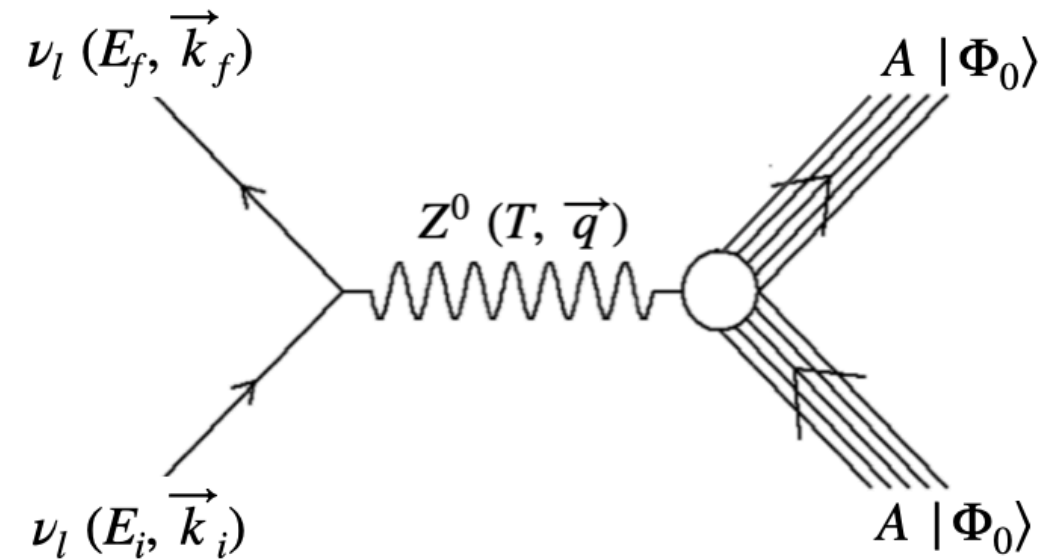
$$Q_W^2 = [g_n^V N + g_p^V Z]^2$$

CEvNS Cross Section and Form Factors

■ Cross section:

$$\frac{d\sigma}{dT} = \frac{G_F^2}{\pi} M_A \left[1 - \frac{T}{E_i} - \frac{M_A T}{2E_i^2} \right] \frac{Q_W^2}{4} F_W^2(q)$$

$$\frac{d\sigma}{d\cos\theta_f} = \frac{G_F^2}{2\pi} E_i^2 (1 + \cos\theta_f) \frac{Q_W^2}{4} F_W^2(q)$$



$$T \in \left[0, \frac{2E_i^2}{(M_A + 2E_i)} \right]$$

$$Q_W^2 = [g_n^V N + g_p^V Z]^2$$

■ Weak Form Factor:

$$\begin{aligned} Q_W F_W(q) &\approx \langle \Phi_0 | \hat{J}_0(q) | \Phi_0 \rangle \\ &\approx (1 - 4 \sin^2 \theta_W) Z F_p(q) - N F_n(q) \\ &\approx 2\pi \int d^3r \left[(1 - 4 \sin^2 \theta_W) \rho_p(r) - \rho_n(r) \right] j_0(qr) \end{aligned}$$

Charge density and charge form factor: proton densities and charge form factors are well known through decades of elastic electron scattering experiments.

Neutron densities and neutron form factor: neutron densities and form factors are poorly known. Note that CEvNS is primarily sensitive to neutron density distributions.

■ Neutron densities and form factor

- Hadronic probes have been used to extract neutron distributions but these measurements are plagued by ill-controlled model-dependent uncertainties associated with the strong interaction.
- Electroweak probes such as parity-violating electron scattering (PVES) and CEvNS provide relatively model-independent ways of determining neutron distributions.

CEvNS Cross Section and Form Factors

■ Neutron densities and form factor

- **Hadronic probes** have been used to extract neutron distributions but these measurements are plagued by ill-controlled model-dependent uncertainties associated with the strong interaction.
- **Electroweak probes** such as parity-violating electron scattering (**PVES**) and **CEvNS** provide relatively model-independent ways of determining neutron distributions.
 - **PVES experiments**: In recent years, PREX experiment at Jefferson lab has measured the weak charge of ^{208}Pb at a single value of momentum transfer, while a follow up PREX-II experiment is underway. CREX experiment at Jefferson lab is underway to measure the weak form factor of ^{48}Ca . PVES experiments are typically carried out at a signal moment transfer.

$$A_{PV}(q^2) = \frac{G_F q^2}{4\pi\alpha\sqrt{2}} \frac{Q_W F_W(q^2)}{Z F_{ch}(q^2)}$$

- **CEvNS experiments**: precise measurement of CEvNS cross section in future ton and multi-ton CEvNS detectors will provide constraints on neutron density distributions and weak form factors of nuclei at low momentum transfers.

$$\frac{d\sigma}{dT} = \frac{G_F^2}{4\pi} M_A \left[1 - \frac{T}{E_i} - \frac{M_A T}{2E_i^2} \right] Q_W^2 F_W^2(q)$$

CEvNS Cross Section: Experimental Status

COHERENT Collaboration at SNS at ORNL

■ Csl:14.6 kg

- Flux averaged cross section extracted

CEvNS cross section	$169^{+30}_{-26} \times 10^{-40} \text{ cm}^2$
SM cross section	$189 \pm 6 \times 10^{-40} \text{ cm}^2$

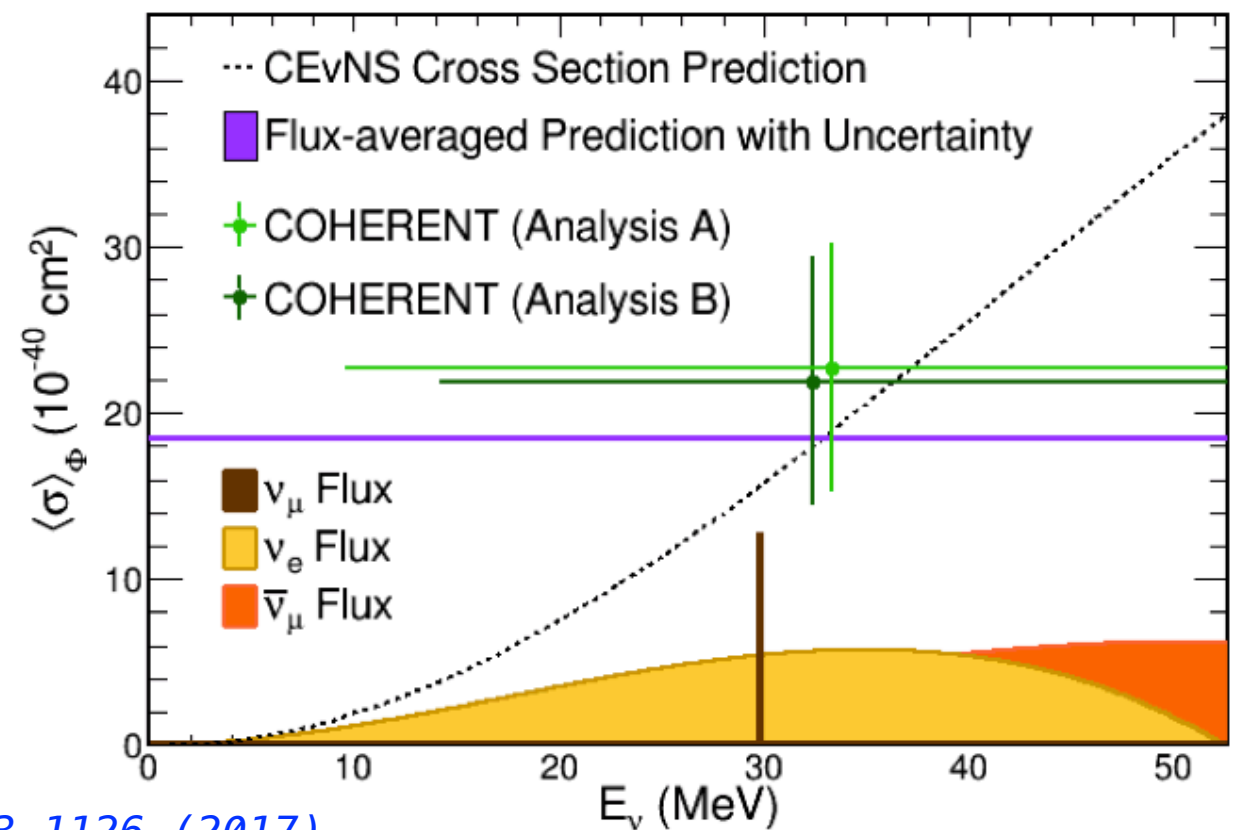
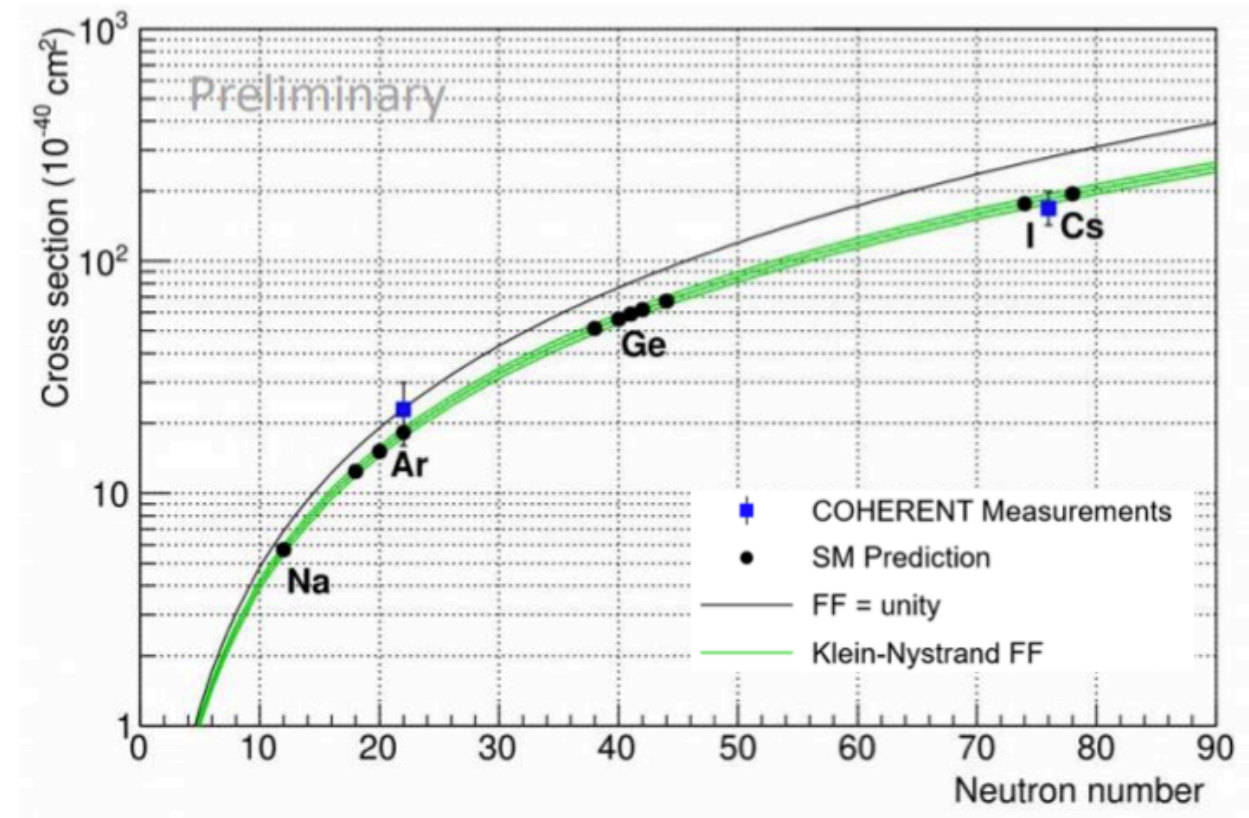
- Systematic uncertainty reduced from 28% (2017 results) to 13% (2020 results in M7 workshop)
- Detector decommissioned

■ ^{40}Ar : CENNS-10, 24 kg

- Flux averaged cross section extracted

$$(2.3 \pm 0.7) \times 10^{-39} \text{ cm}^2$$

- Collecting more data



D. Akimov et al. [COHERENT], Science 357, 6356, 1123–1126 (2017)

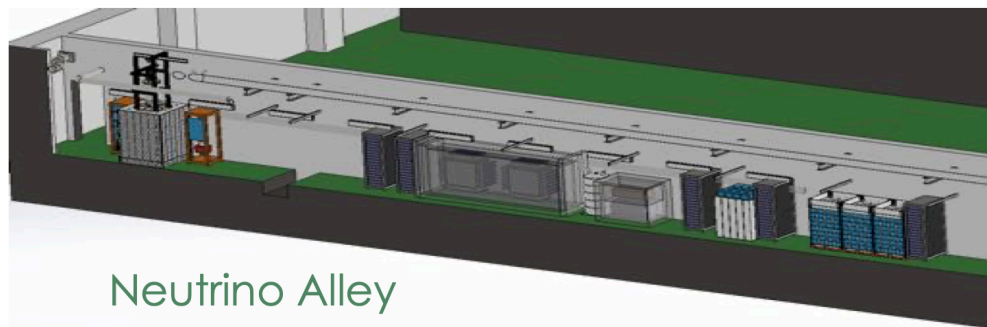
D. Akimov et al. [COHERENT], arXiv:2003.10630 [nucl-ex]

CEvNS: Ton-Scale LAr Detectors

COHERENT

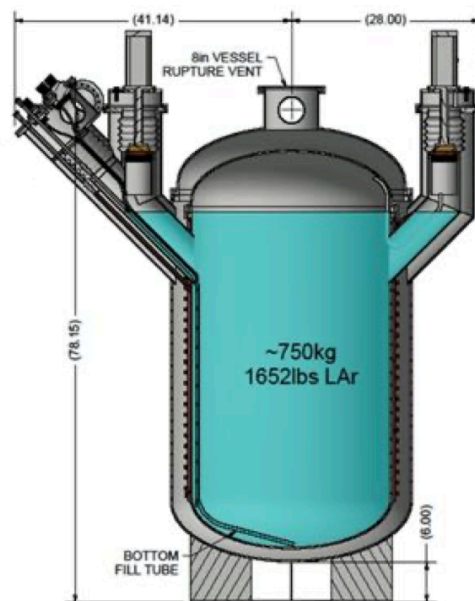
750kg LAr detector at SNS at ORNL

- In R&D phase.



Neutrino Alley

High Statistics CEvNS



Walt Fox, IU

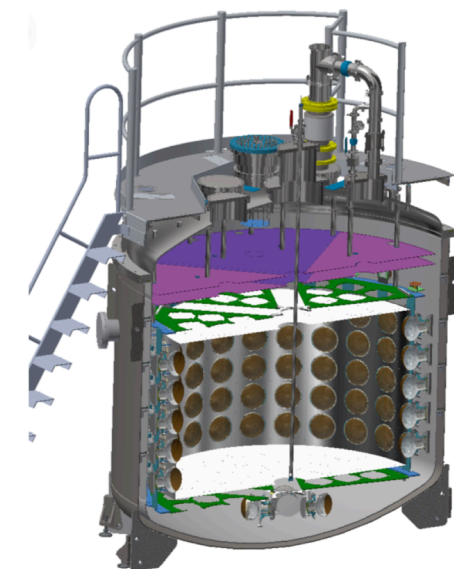
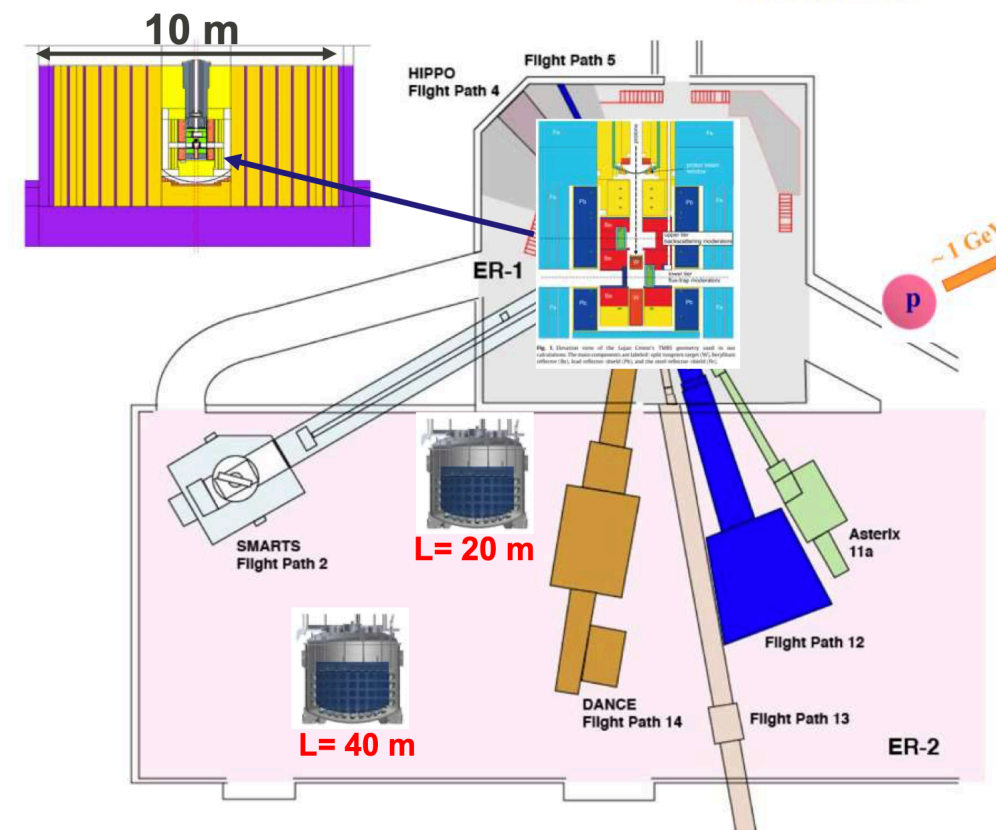
- 750kg LAr
- Single phase
- Light Collection Options
 - 3" PMT TPB
 - SiPM, Xenon Doping, ...
- ~3000 CEvNS/yr

Jason Newby, Neutrino 2020

Coherent CAPTAIN-Mills (CCM)

10 ton LAr detector at Lujan center at LANL

- Collected data in 2019, analysis ongoing
- Detector is being upgraded, will collect more data in summer 2021

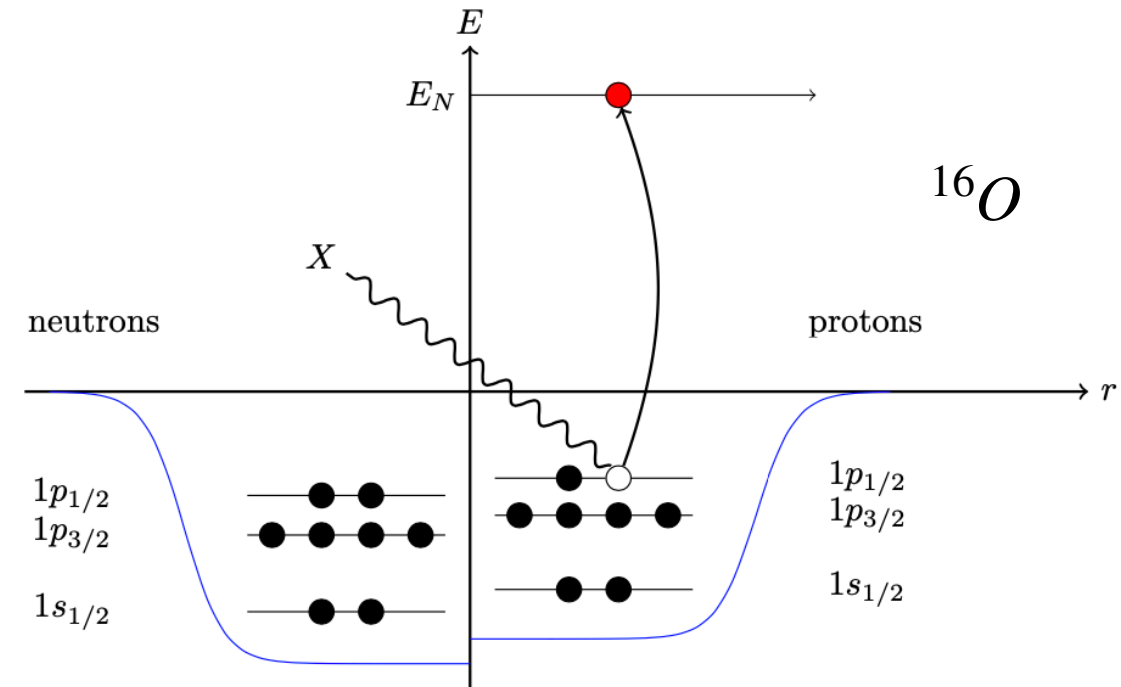


CEvNS Cross Section: HF-SkE2 Model

- A microscopic many-body nuclear theory model.
- Nuclear ground state is described as a many-body quantum mechanical system where nucleons are bound in an effective nuclear potential.
- Solve Hartree-Fock (HF) equation with a Skyrme (SkE2) nuclear potential to obtain single-nucleon wave functions for the bound nucleons in the nuclear ground state. Fill up nuclear shells following Pauli principle.
- Evaluate proton and neutron density distributions from those wave functions:

$$\rho_{\tau}(r) = \frac{1}{4\pi r^2} \sum_{\alpha} v_{\alpha,\tau}^2 (2j_{\alpha} + 1) |\phi_{\alpha,\tau}(r)|^2 \quad (\tau = p, n)$$

$$(\alpha \in n_{\alpha}, l_{\alpha}, j_{\alpha})$$

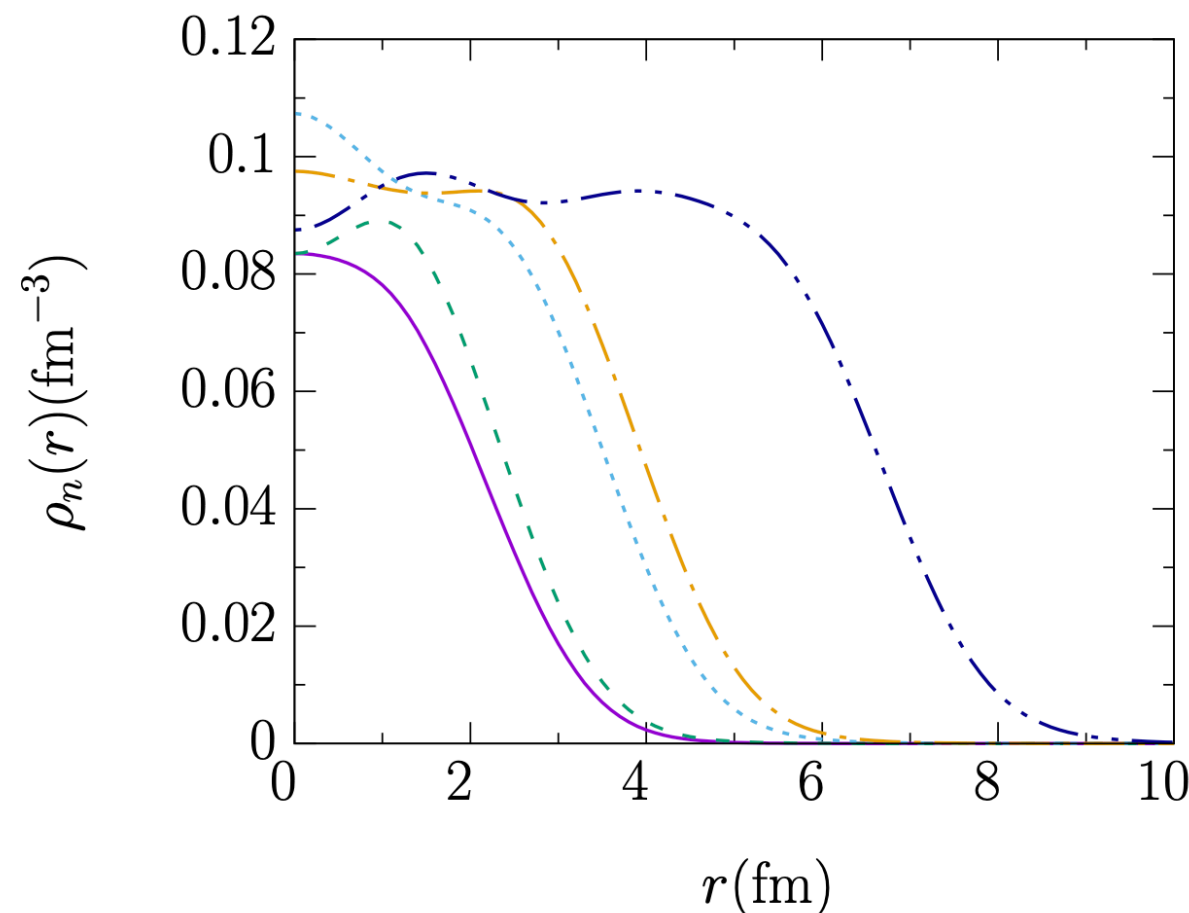
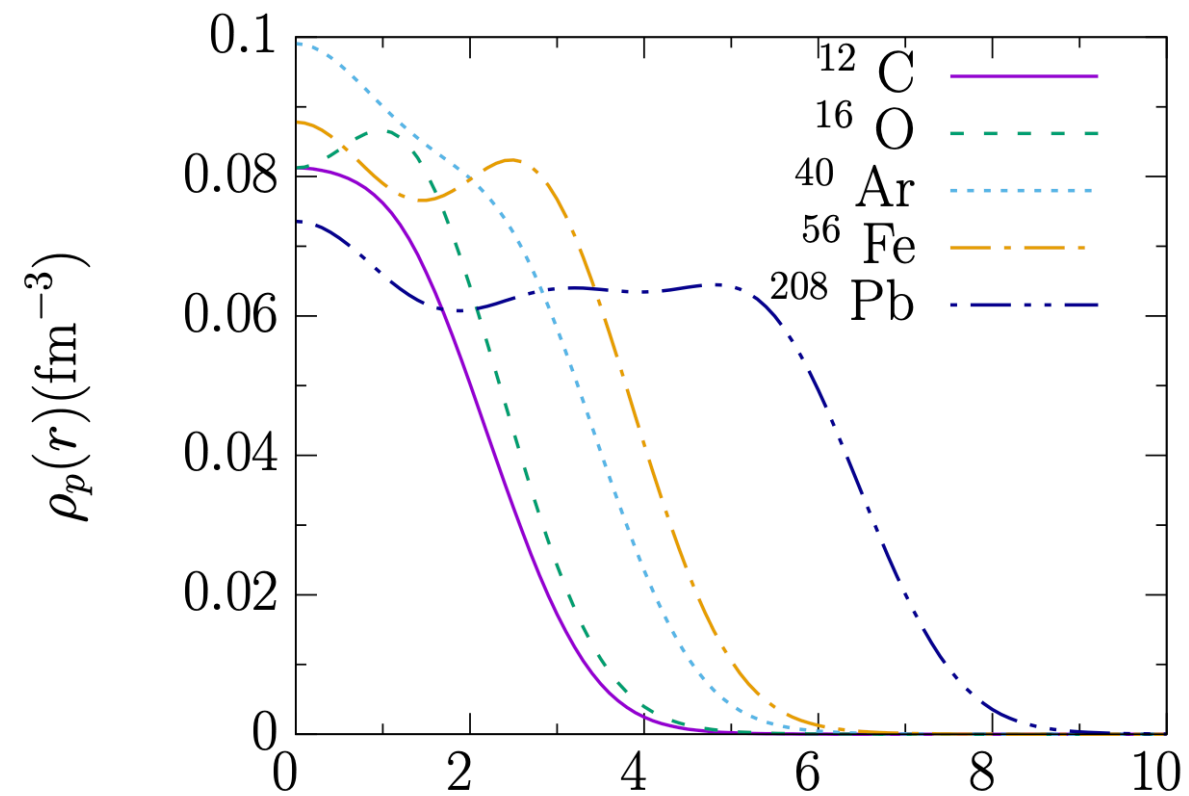


CEvNS Cross Section: HF-SkE2 Model

- A microscopic many-body nuclear theory model.
- Nuclear ground state is described as a many-body quantum mechanical system where nucleons are bound in an effective nuclear potential.
- Solve Hartree-Fock (**HF**) equation with a Skyrme (**SkE2**) nuclear potential to obtain **single-nucleon wave functions** for the bound nucleons in the nuclear ground state. Fill up nuclear shells following Pauli principle.
- Evaluate proton and neutron density distributions from those wave functions:

$$\rho_{\tau}(r) = \frac{1}{4\pi r^2} \sum_{\alpha} v_{\alpha,\tau}^2 (2j_{\alpha} + 1) |\phi_{\alpha,\tau}(r)|^2 \quad (\tau = p, n)$$

$(\alpha \in n_{\alpha}, l_{\alpha}, j_{\alpha})$



CEvNS Cross Section: HF-SkE2 Model

- A microscopic many-body nuclear theory model.
- Nuclear ground state is described as a many-body quantum mechanical system where nucleons are bound in an effective nuclear potential.
- Solve Hartree-Fock (**HF**) equation with a Skyrme (**SkE2**) nuclear potential to obtain **single-nucleon wave functions** for the bound nucleons in the nuclear ground state. Fill up nuclear shells following Pauli principle.
- Evaluate proton and neutron density distributions from those wave functions:

$$\rho_{\tau}(r) = \frac{1}{4\pi r^2} \sum_{\alpha} v_{\alpha,\tau}^2 (2j_{\alpha} + 1) |\phi_{\alpha,\tau}(r)|^2 \quad (\tau = p, n)$$

$(\alpha \in n_{\alpha}, l_{\alpha}, j_{\alpha})$

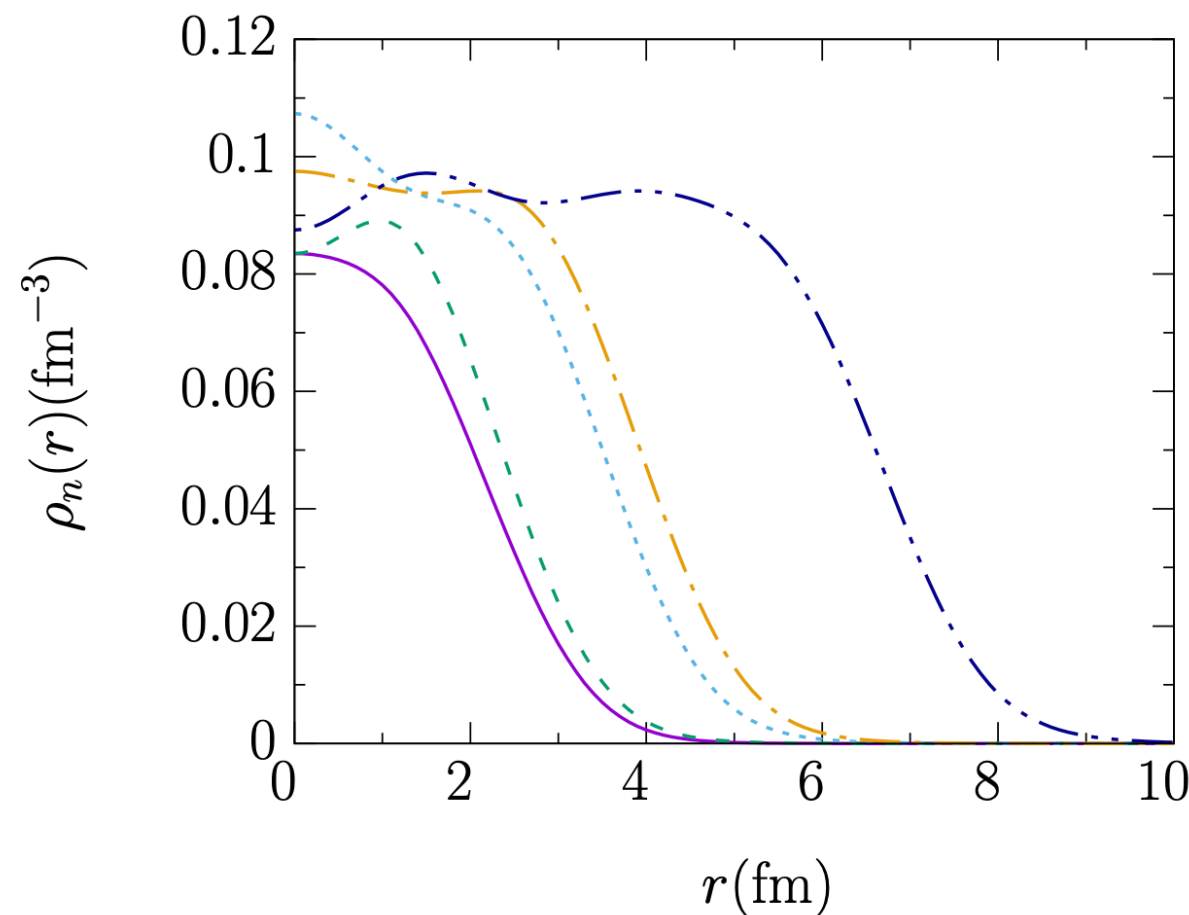
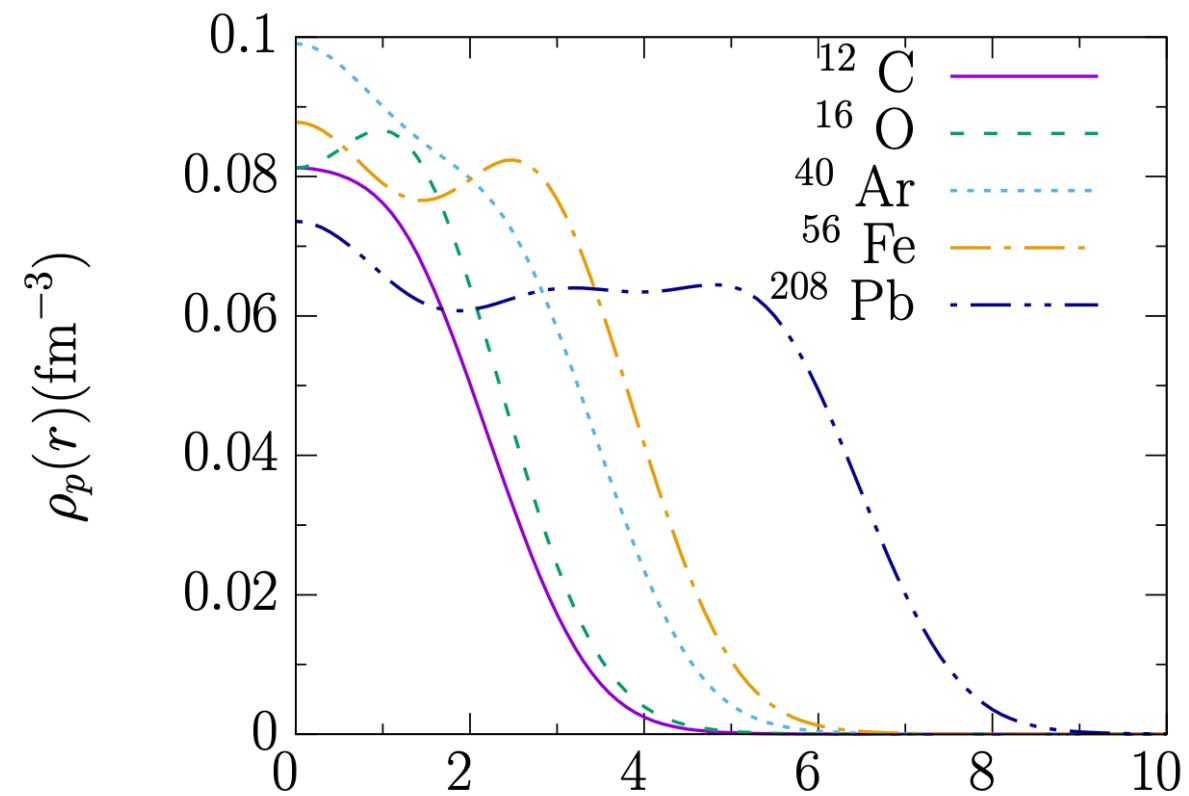
- The proton and neutron densities are utilized to calculate proton and neutron form factors:

$$F_n(q) = \frac{1}{N} \int d^3r j_0(qr) \rho_n(r)$$

$$F_p(q) = \frac{1}{Z} \int d^3r j_0(qr) \rho_p(r)$$

$$N = \int d^3r \rho_n(r)$$

$$Z = \int d^3r \rho_p(r)$$

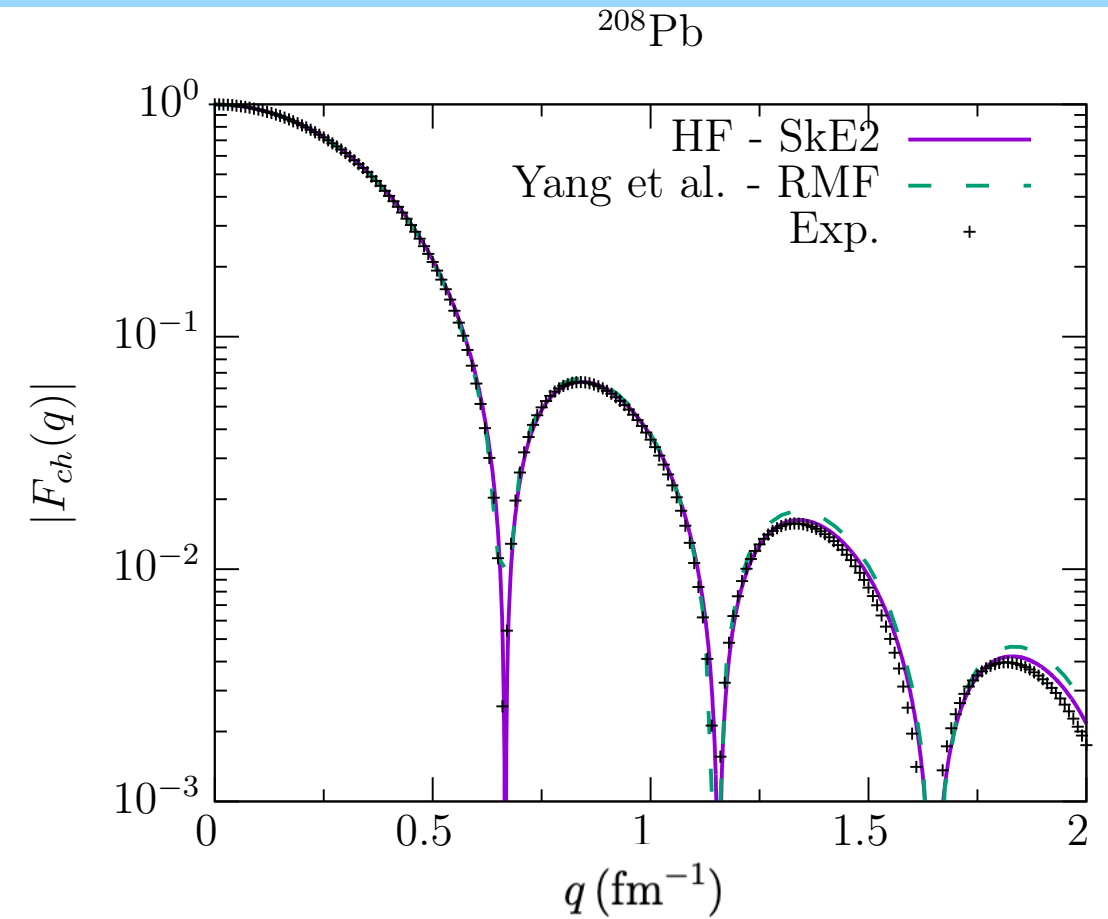


HF-SkE2 Model: ^{208}Pb Results

■ Charge Form Factor

- Our charge form factor predictions of ^{208}Pb describe the elastic electron scattering experimental data remarkably well.

*Experimental data from:
H. De Vries, et al., Atom. Data Nucl. Data Tabl. 36, 495 (1987)*



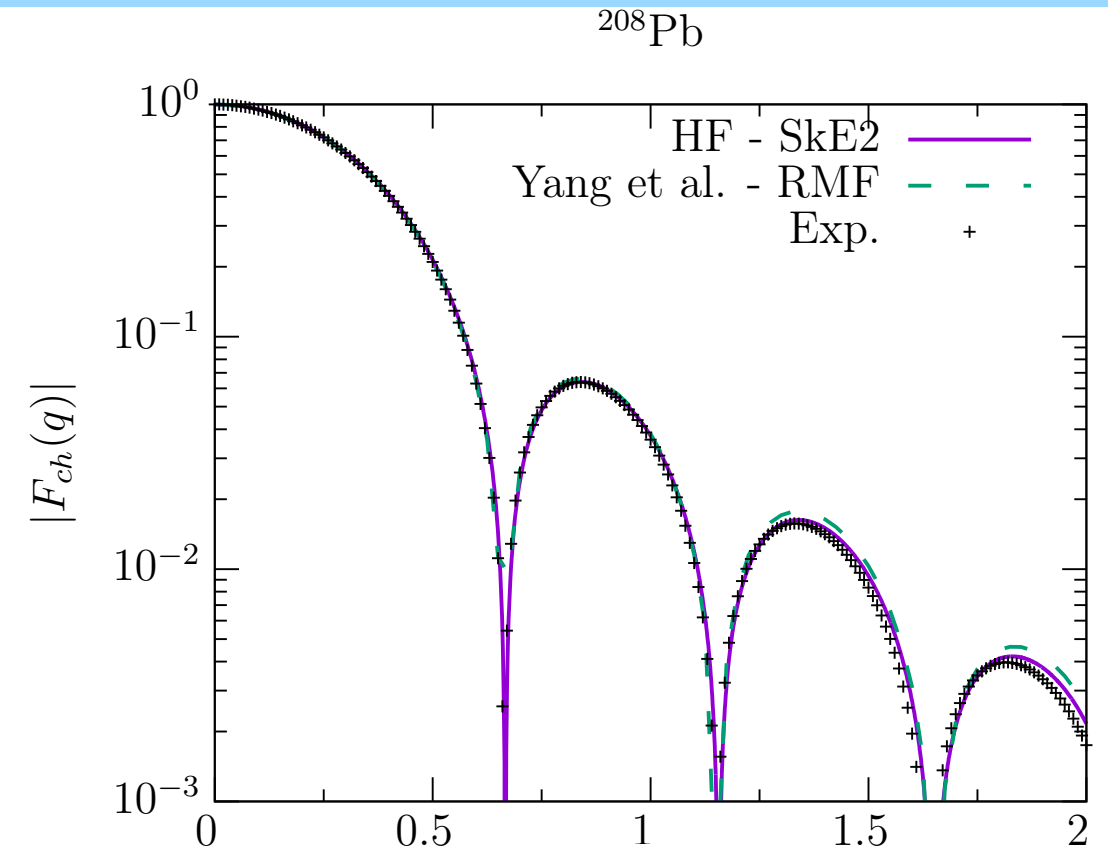
HF-SkE2 Model: ^{208}Pb Results

■ Charge Form Factor

- Our charge form factor predictions of ^{208}Pb describe the elastic electron scattering experimental data remarkably well.

Experimental data from:

H. De Vries, et al., Atom. Data Nucl. Data Tabl. 36, 495 (1987)



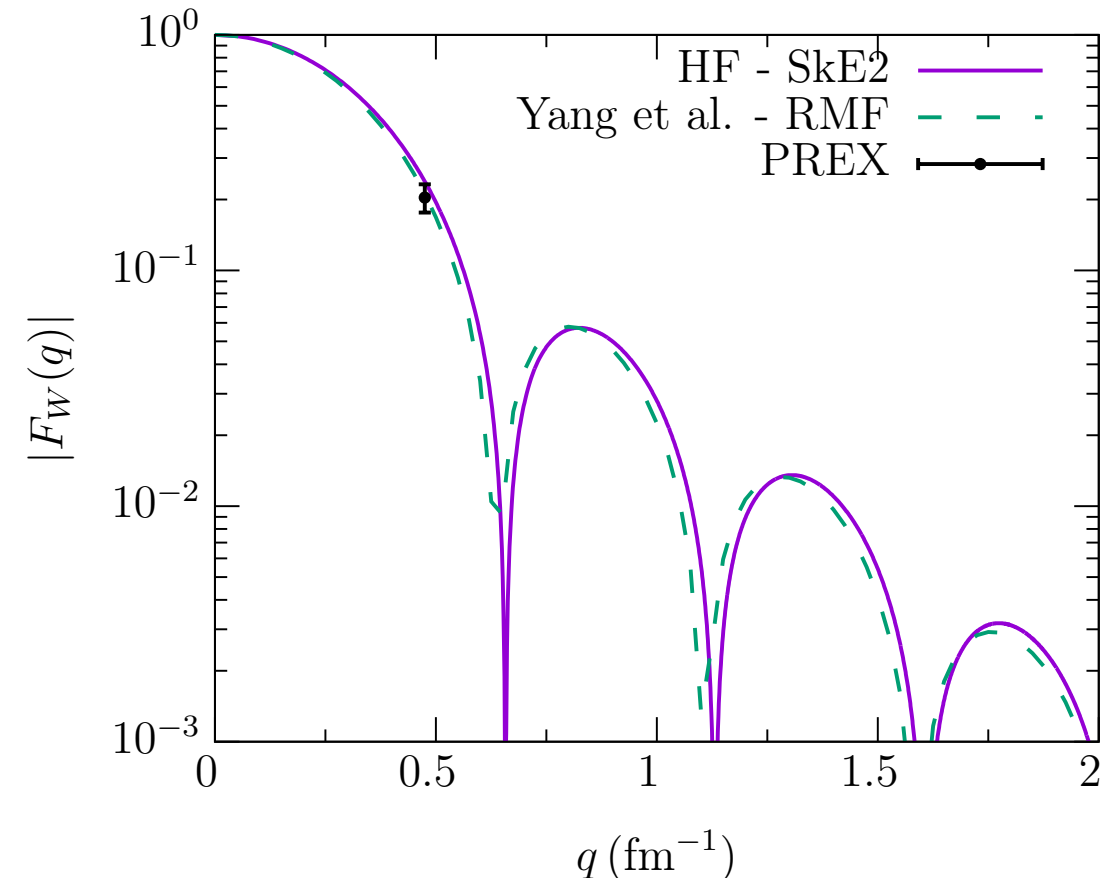
■ Weak Form Factor

- Weak form factor predictions shown along with the single data point measured by the PREX collaboration at a momentum transfer of $q = 0.475 \text{ fm}^{-1}$.
- The follow-up PREX-II measurement at Jefferson lab aims to reduce the error bars by at least a factor of three.

PREX data from:

- S. Abrahamyan et al., Phys. Rev. Lett. 108, 112502 (2012).

- C. J. Horowitz et al., Phys. Rev. C 85, 032501 (2012).



- Both calculations compared with RMF predictions of Yang et al. (*Phys. Rev. C 100, 054301 (2019)*).

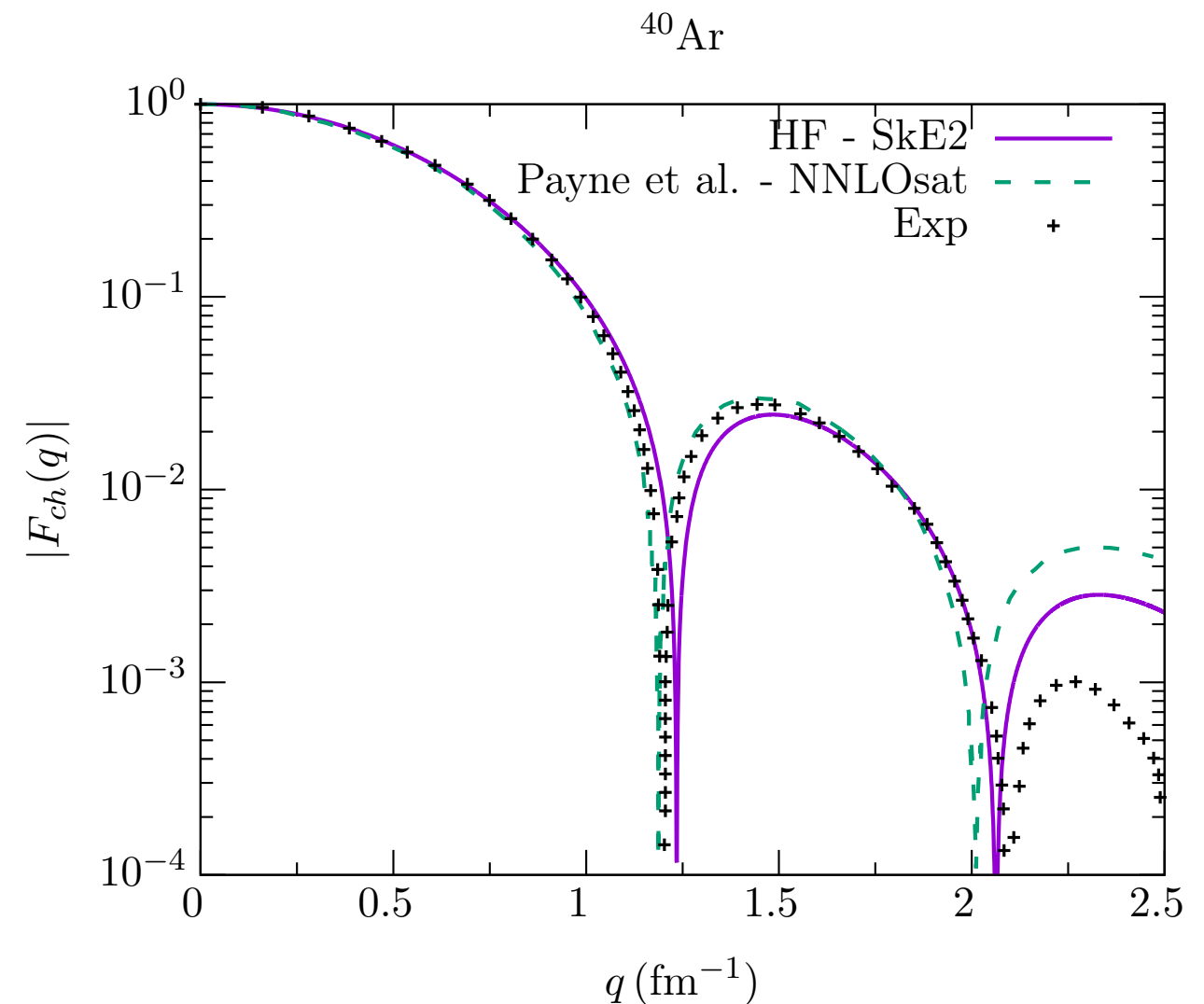
Constraining ^{40}Ar form factor and CEvNS cross section

■ Charge Form Factor

- The ^{40}Ar charge form factor predictions describe experimental elastic electron scattering data well for $q < 2 \text{ fm}^{-1}$.
- For energies relevant for pion decay-at-rest neutrinos, the region above $q > 0.5 \text{ fm}^{-1}$ does not contribute to CEvNS cross section.

Experimental data from:

C. R. Ottermann et al., Nucl. Phys. A 379, 396 (1982).

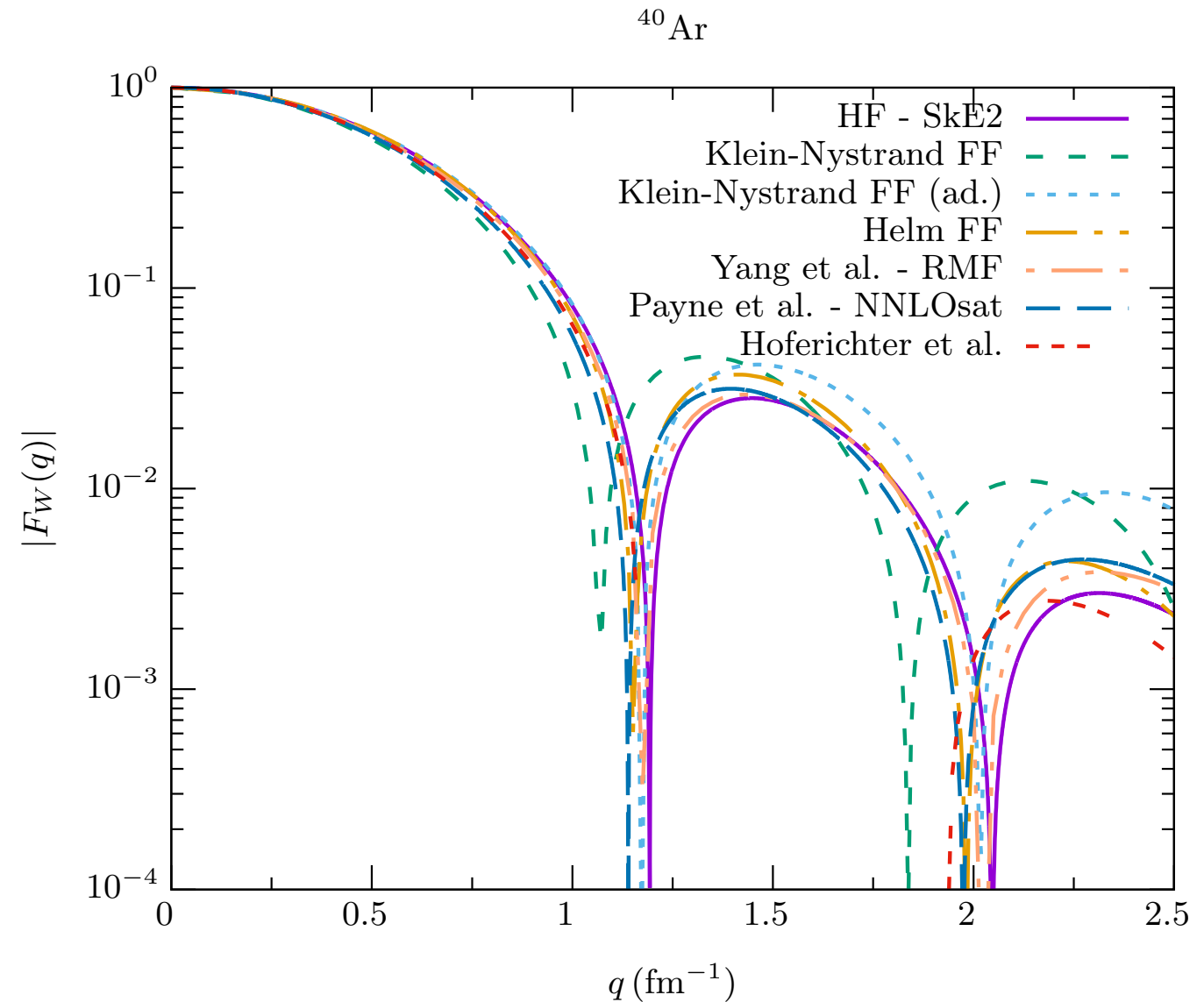


- Our calculations compared with Payne *et al.* [Phys. Rev. C 100, 061304 (2019)] where form factors are calculated within a coupled-cluster theory from first principles using a chiral NNLO_{sat} interaction.

Constraining ^{40}Ar form factor and CEvNS cross section

■ Weak Form Factor

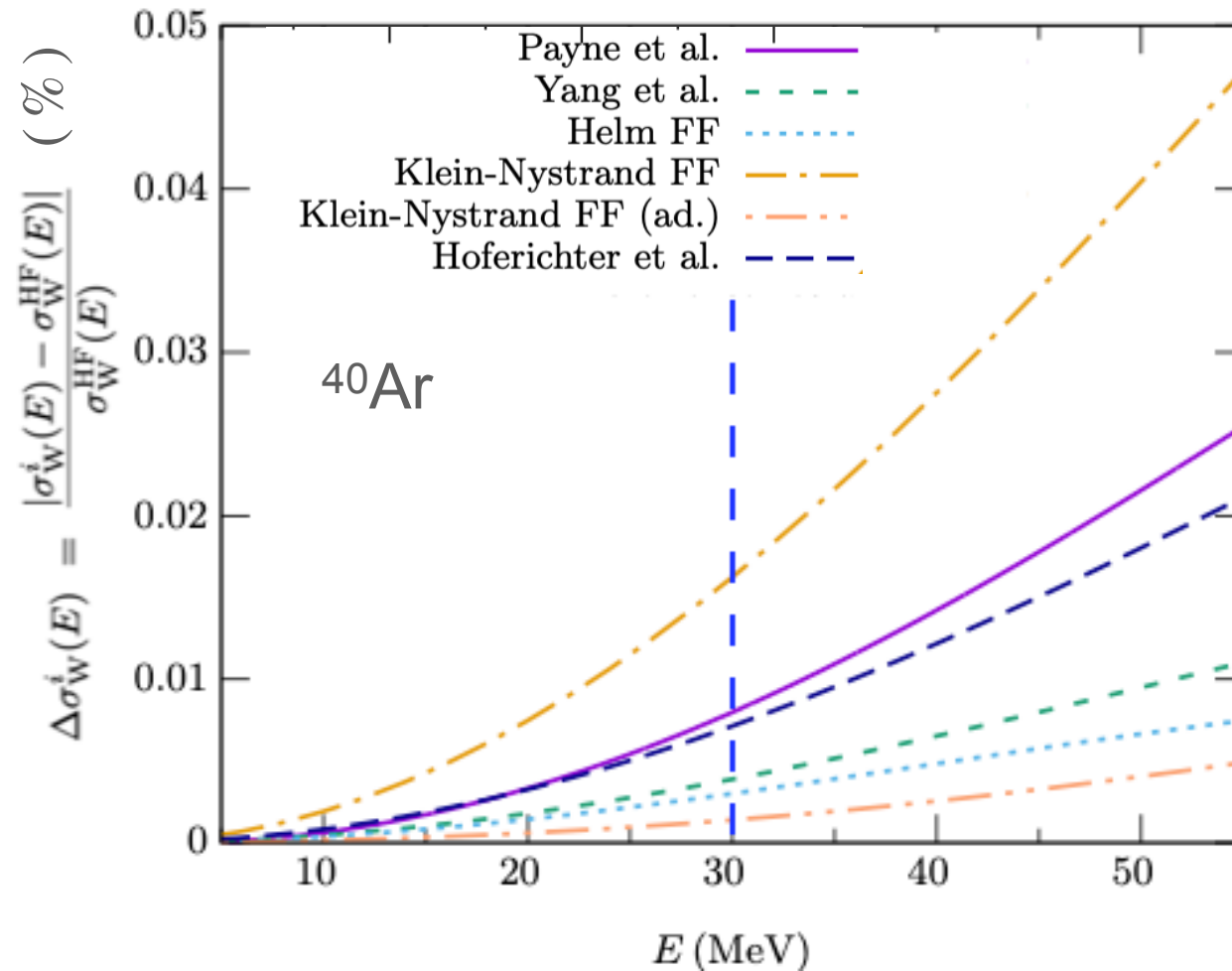
- Comparison of ^{40}Ar form factor predictions from **four nuclear theory** and **three phenomenological calculations**.
- Different approaches are based on different representations of the nuclear densities.



- The *HF-SkE2* model [[arXiv:2007.03658](https://arxiv.org/abs/2007.03658) [nucl-th]]
- Model of *Payne et al.* [[Phys. Rev. C 100, 061304 \(2019\)](https://doi.org/10.1103/PhysRevC.100.061304)] where form factors are calculated within a coupled-cluster theory from first principles using a chiral NNLO_{sat} interaction.
- Model of *Yang et al.* [[Phys. Rev. C 100, 054301 \(2019\)](https://doi.org/10.1103/PhysRevC.100.054301)] where form factors are predicted within a relativistic mean-field model informed by the properties of finite nuclei and neutron stars.
- Model of *Hoferichter et al.* [[Phys. Rev. D 102, 074018 \(2020\)](https://doi.org/10.1103/PhysRevD.102.074018)] where form factors are calculated within a large-scale nuclear shell model.
- *Helm and Klein-Nystrand* [adapted by COHERENT] predictions

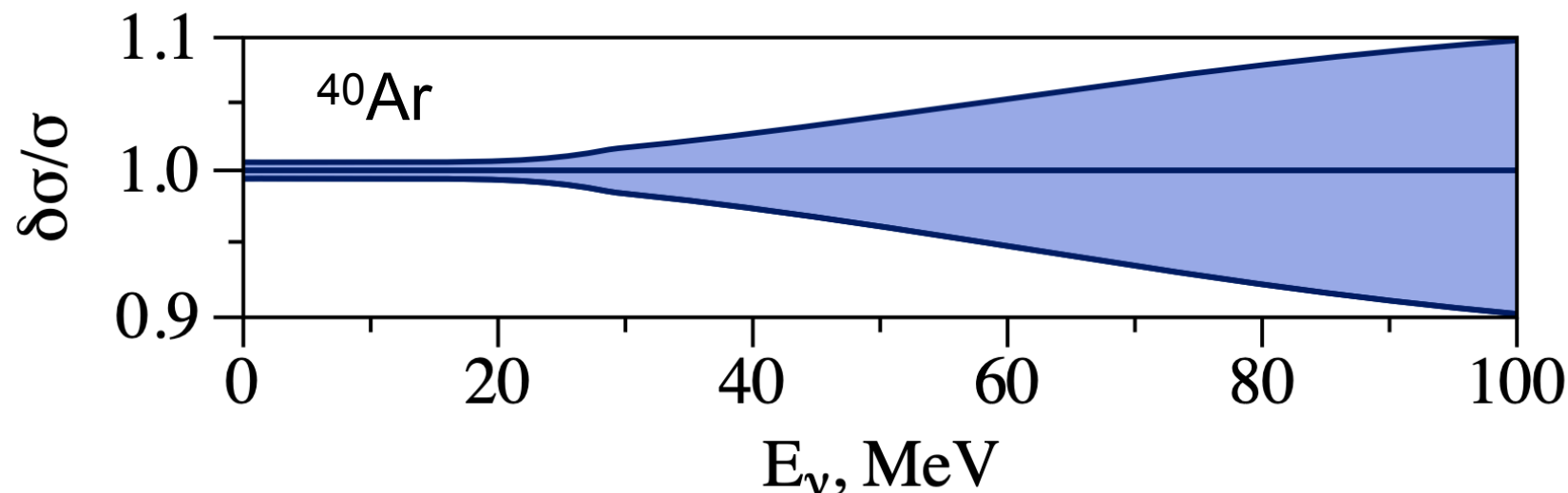
Constraining ^{40}Ar form factor and CEvNS cross section

- Relative CEvNS cross section differences between the results of different calculations:



N. Van Dessel, V. Pandey, H. Ray, N. Jachowicz, arXiv:2007.03658 [nucl-th]

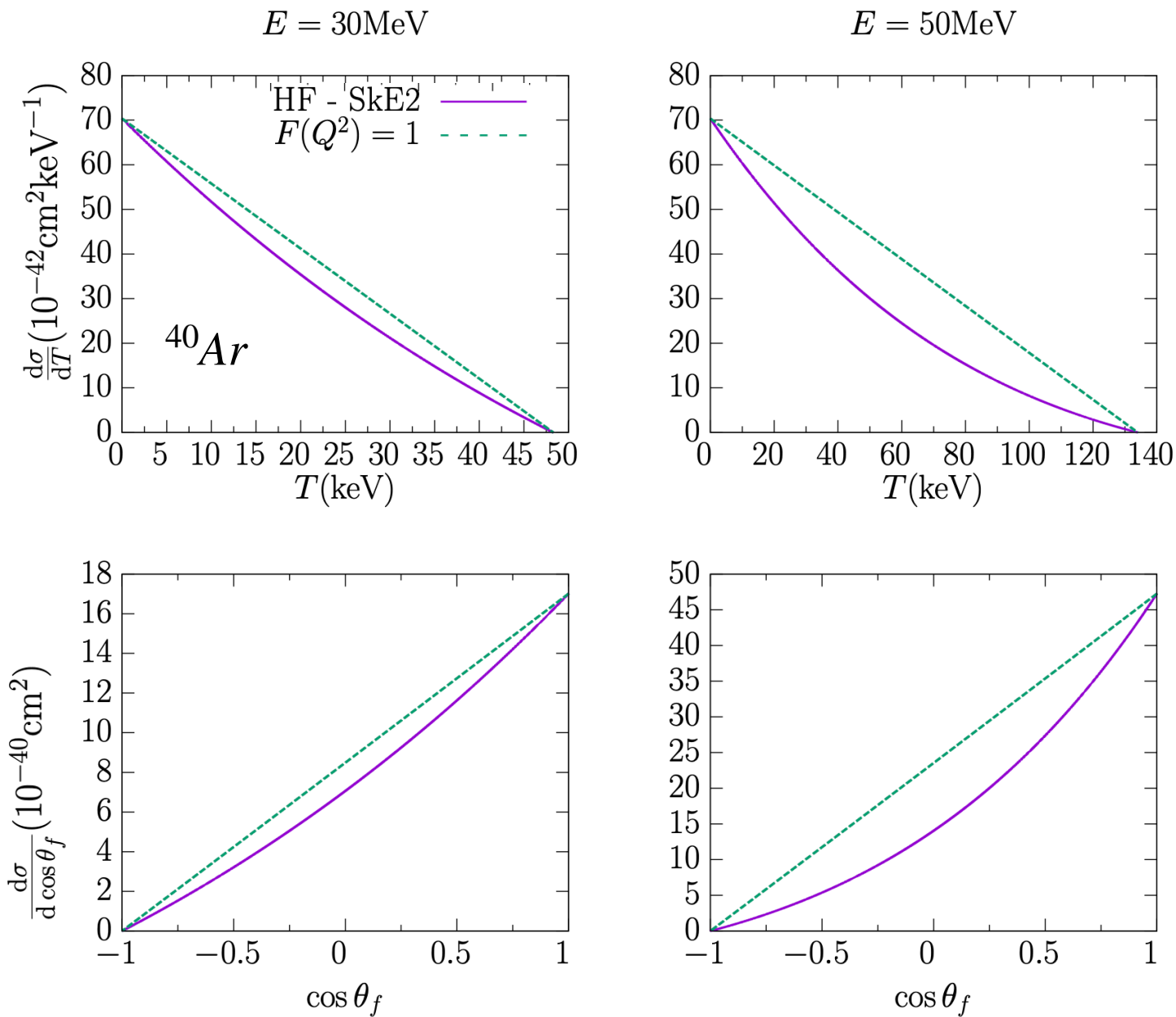
- Relative CEvNS cross section theoretical uncertainty (includes nuclear, nucleonic, hadronic, quark levels as well as perturbative errors):



O. Tomalak, P. Machado, V. Pandey, R. Plestid, arXiv:2011.05960 [hep-ph]

Constraining ^{40}Ar form factor and CEvNS cross section

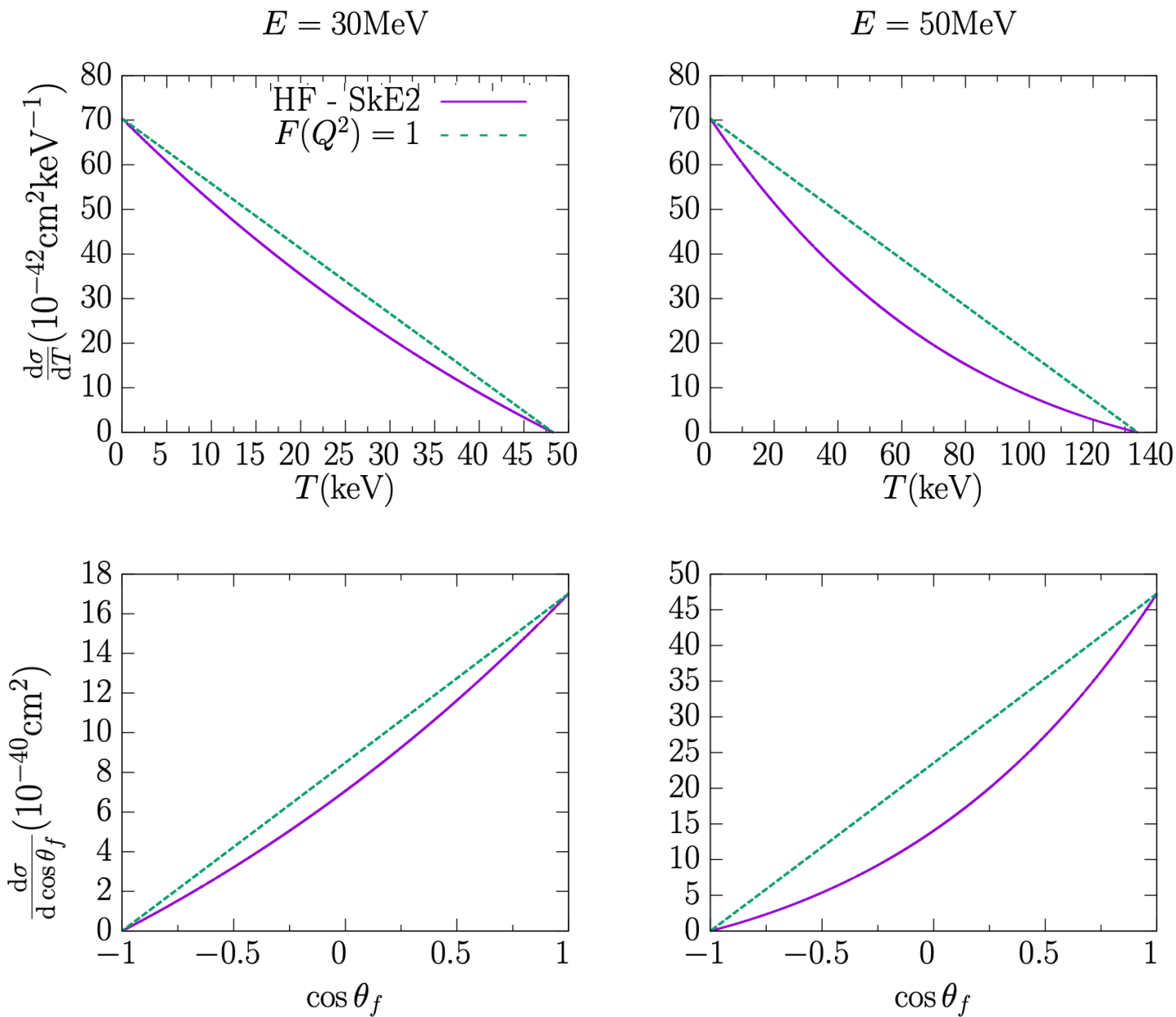
■ Differential cross section:



- Most of the cross section strength lies in the lower-end of the recoil energy and in the forward scattering as the cross section falls off rapidly at higher T and higher θ_f values.
- The effects of nuclear structure physics are more prominent as the neutrino energy increases.

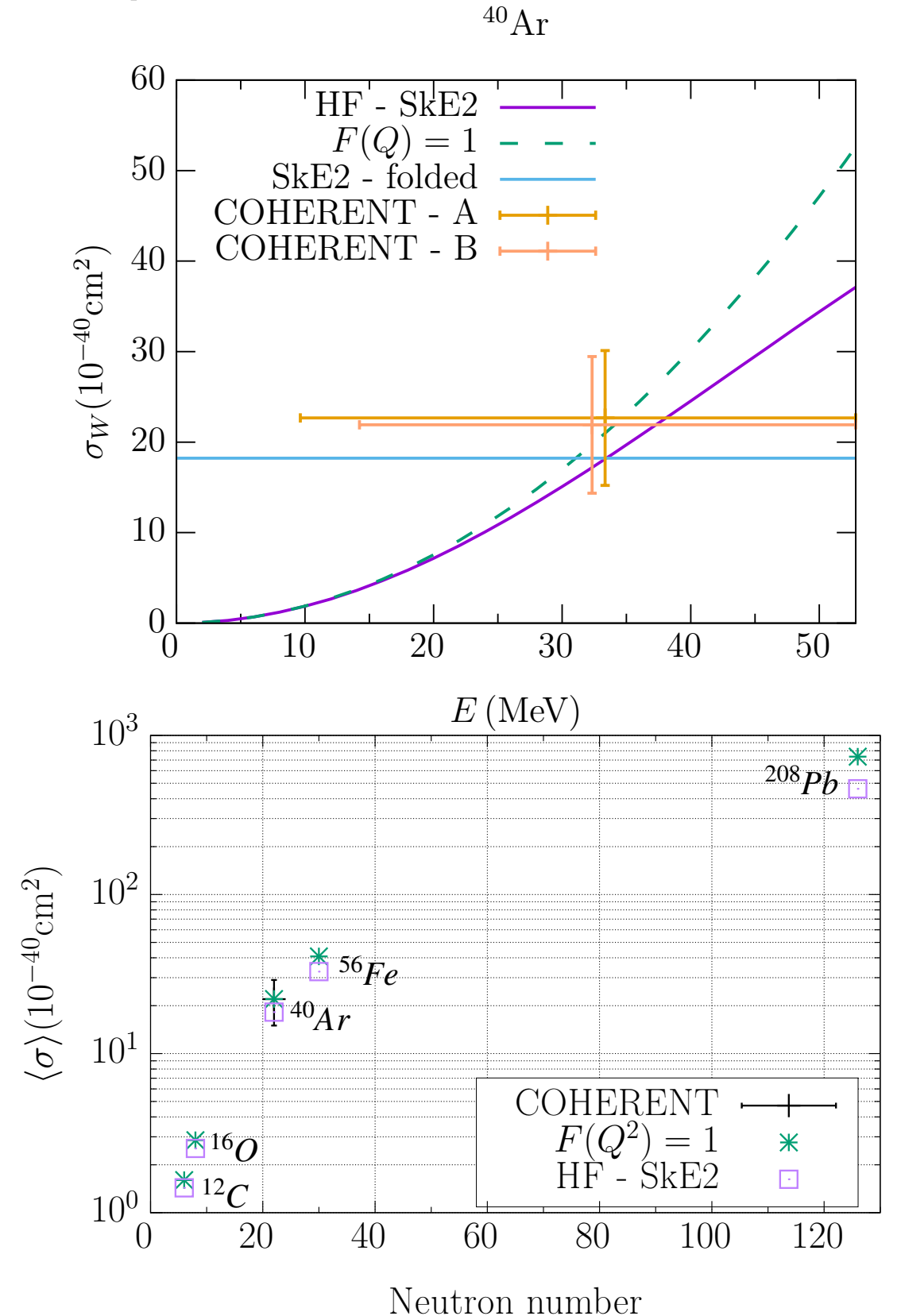
Constraining ^{40}Ar form factor and CEvNS cross section

Differential cross section:



- Most of the cross section strength lies in the lower-end of the recoil energy and in the forward scattering as the cross section falls off rapidly at higher T and higher θ_f values.
- The effects of nuclear structure physics are more prominent as the neutrino energy increases.

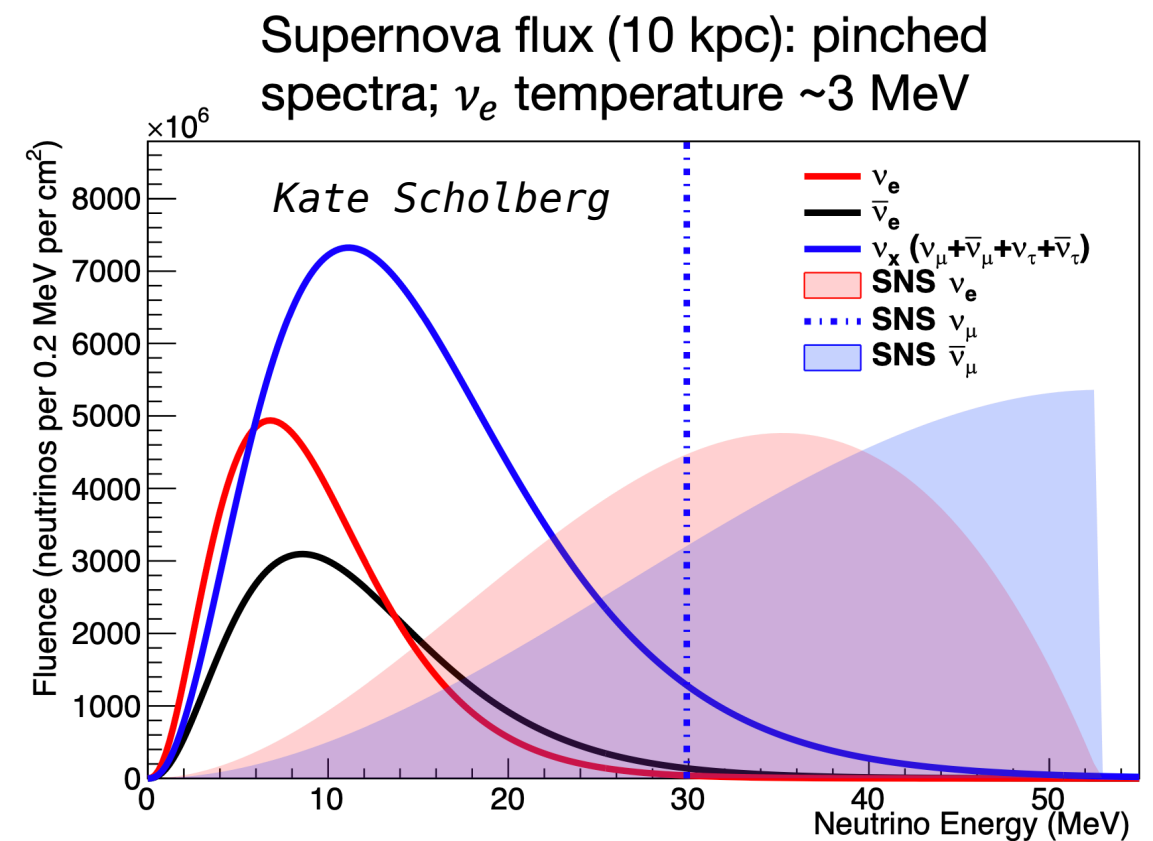
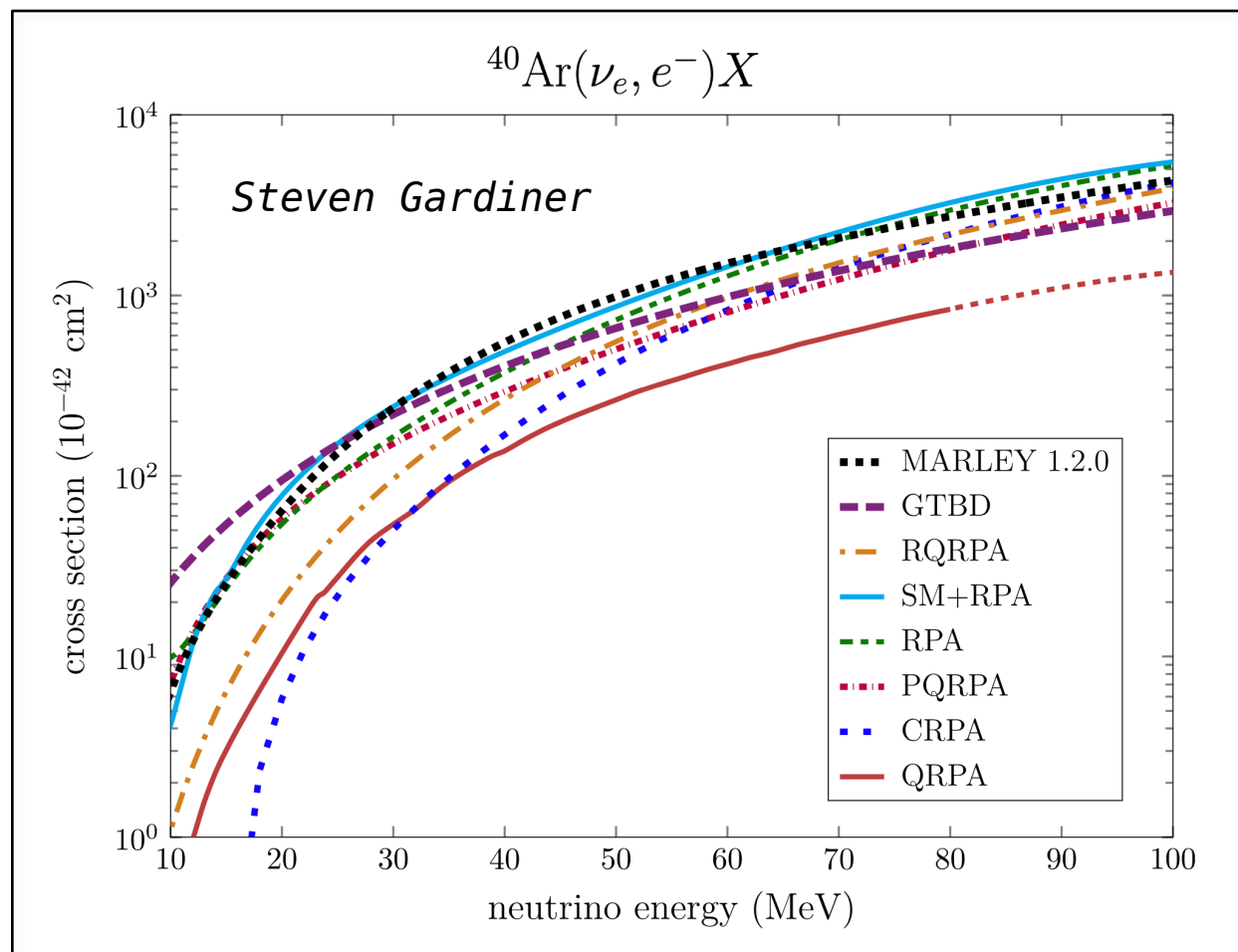
Comparison with COHERENT CENNS-10 data



COHERENT data from:
D. Akimov et al. [COHERENT], arXiv:2003.10630 [nucl-ex].

10s of MeV Inelastic Neutrino-Nucleus Scattering

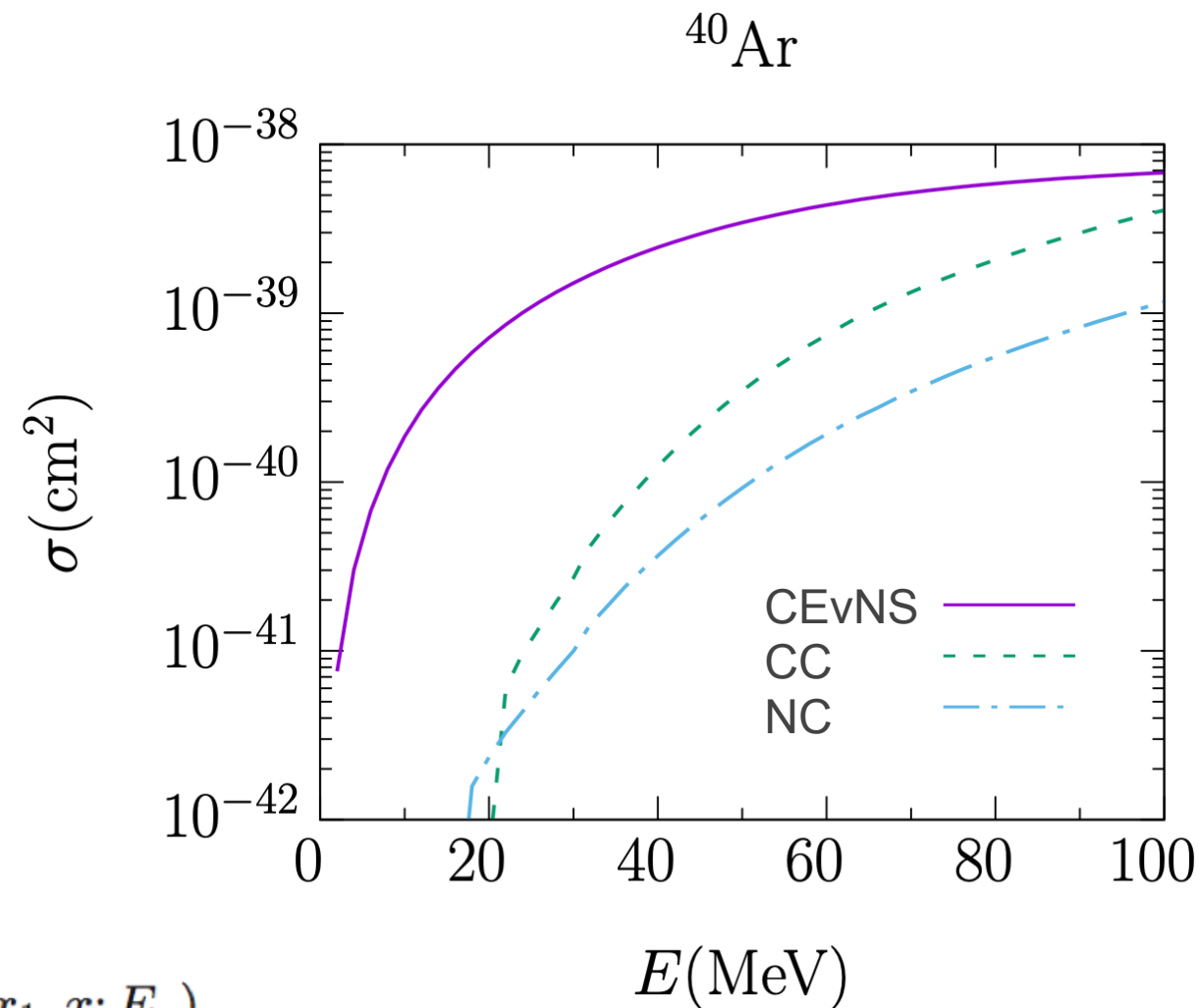
- CEvNS experiments at **stopped-pion sources** are also powerful avenues to measure **10s of MeV inelastic CC and NC** cross sections subject to detailed underlying nuclear structure and dynamics.
 - These are vital in understanding of **core-collapse supernovae**, but are almost completely unexplored experimentally so far.
 - These measurement will greatly enhance the prospects of detecting neutrinos from a core-collapse supernova in future long baseline neutrino experiments.



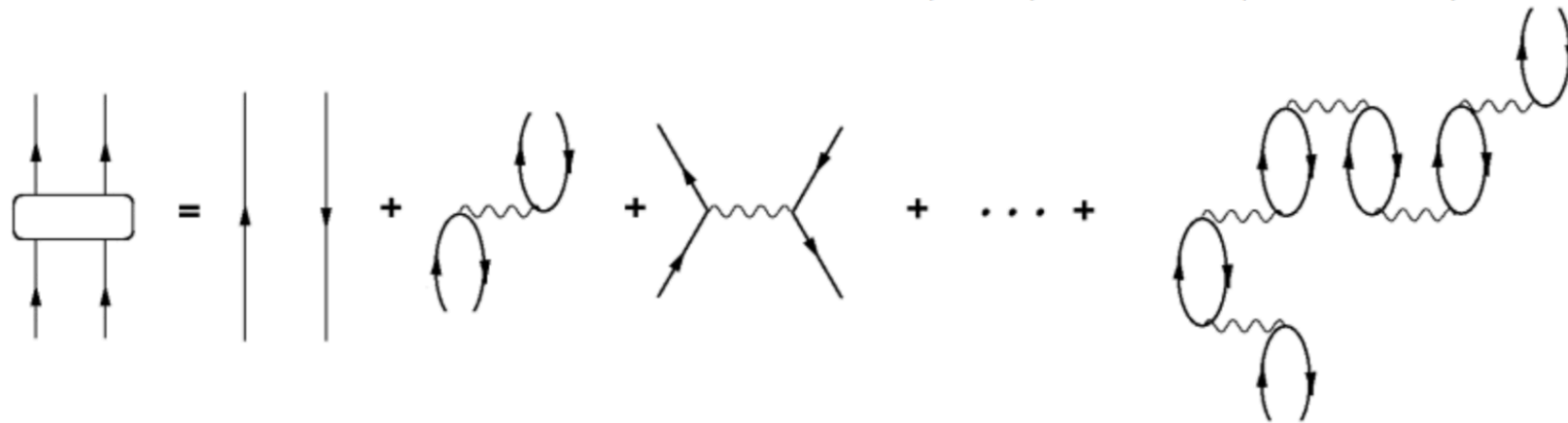
◆ Need inelastic cross section measurements in CEvNS experiments at stopped-pion sources.

Inelastic CC/NC Neutrino-Nucleus Scattering: HF-CRPA Model

- In the inelastic cross section calculations, the influence of long-range correlations between the nucleons is introduced through the **continuum Random Phase Approximation (CRPA)** on top of the HF-SkE2 approach.
- CRPA effects are vital to describe the quasielastic scattering process where the nucleus can be excited to low-lying collective nuclear states.
- The local RPA-polarization propagator is obtained by an iteration to all orders of the first order contribution to the particle-hole Green's function.



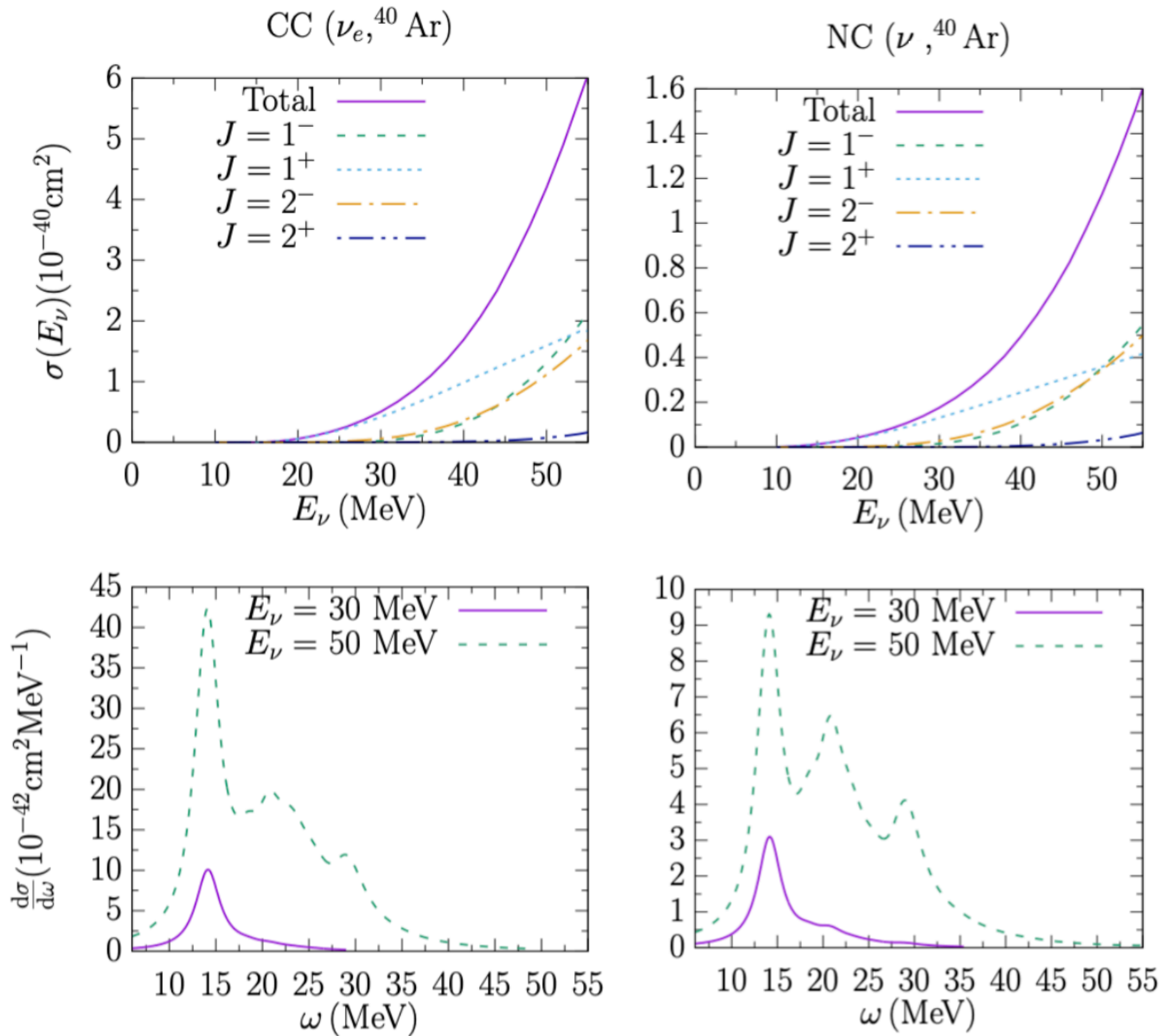
$$\begin{aligned} \Pi^{(RPA)}(x_1, x_2; E_x) &= \Pi^{(0)}(x_1, x_2; E_x) + \frac{1}{\hbar} \int dx dx' \Pi^0(x_1, x; E_x) \\ &\quad \times \tilde{V}(x, x') \Pi^{(RPA)}(x', x_2; E_x) \end{aligned}$$



- More details on CRPA model and other CRPA results:

[arXiv: 2010.05794 \[nucl-th\]](#), *Phys. Rev. C* 101, 045502 (2020), *Phys. Rev. Lett.* 123, 052501 (2019), *Phys. Rev. C* 97, 044616 (2018), *Phys. Rev. C* 94, 054609 (2016), *Phys. Rev. C* 92, 024606 (2015),...

HF-CRPA Model: CC and NC ^{40}Ar Cross Sections

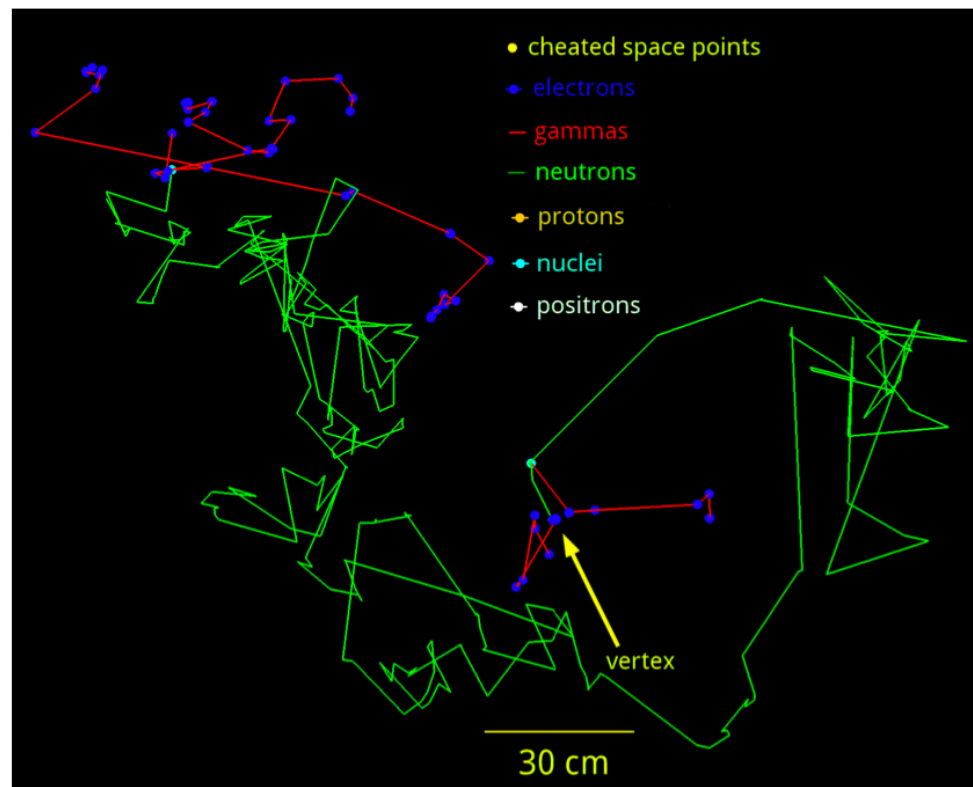


Inelastic CC/NC Neutrino-Nucleus Scattering: MARLEY Generator

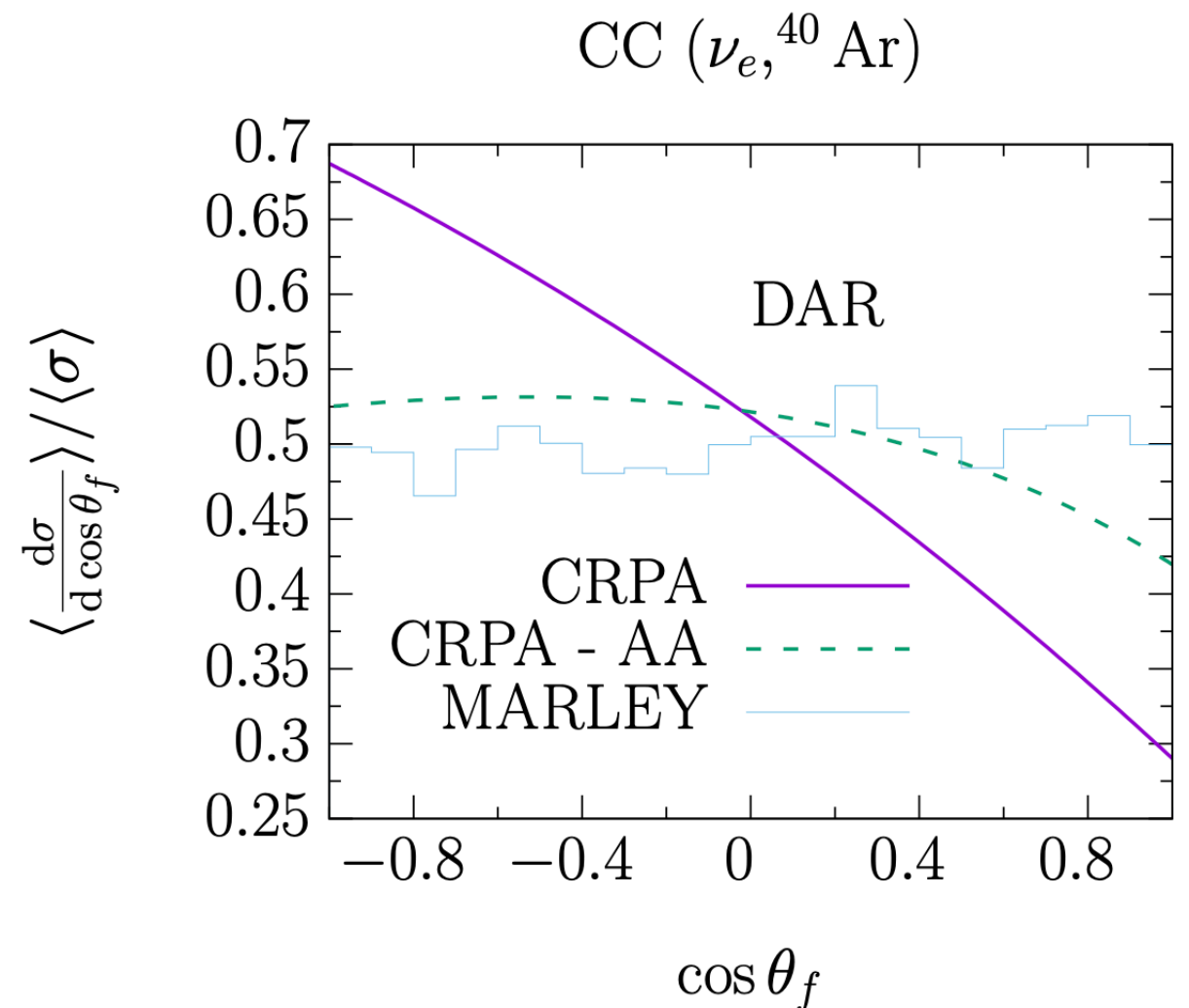
- [MARLEY](#) (Model of Argon Reaction Low Energy Yields) is a neutrino event generator specifically developed to simulate tens-of-MeV neutrino-nucleus interactions in liquid argon.

Steven Gardiner [arXiv:2010.02393 [nucl-th].

- An example of MARLEY ν_e CC event simulated in LArSoft, showing the trajectories and energy deposition points of the interaction products.



arXiv:2008.06647 [hep-ex] [DUNE Collaboration]



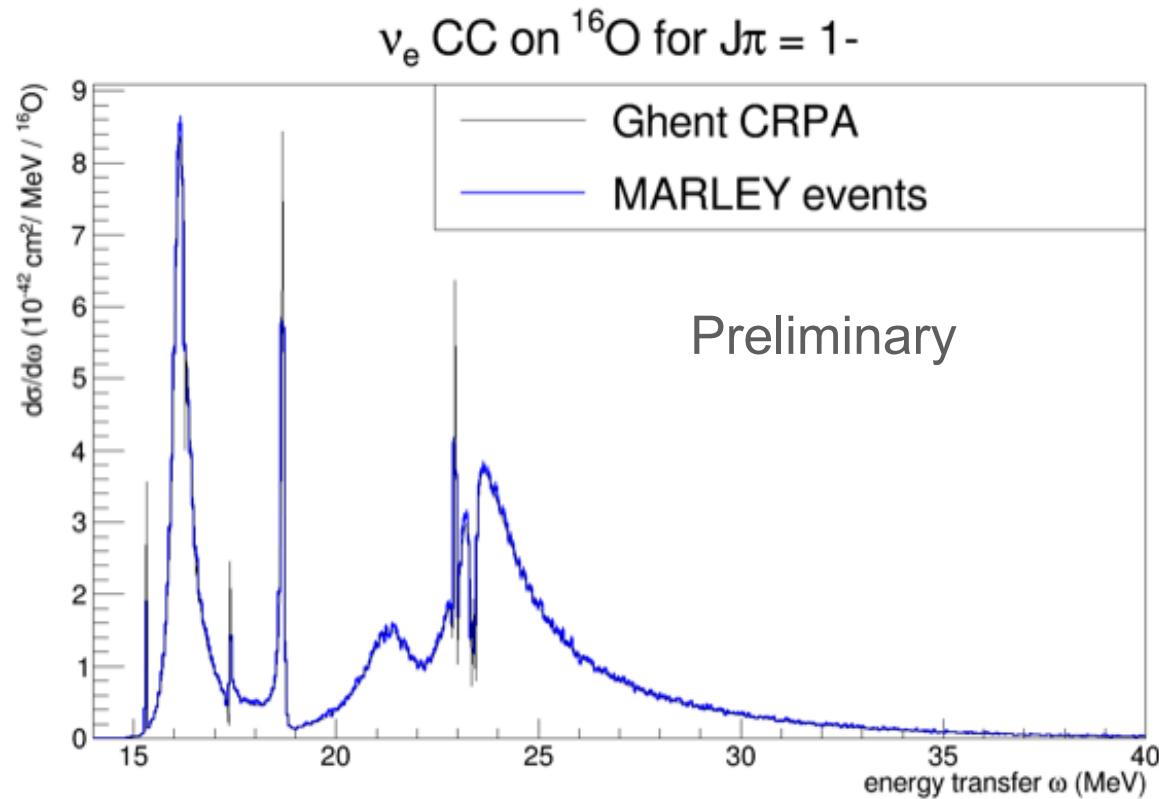
- MARLEY predicts a nearly flat angular distribution (only allowed transitions, Fermi and Gamow Teller strengths).
- CRPA includes full expansion of nuclear matrix element (allowed as well as forbidden transition), predict more backwards strength.

Inelastic CC/NC Neutrino-Nucleus Scattering: MARLEY Generator

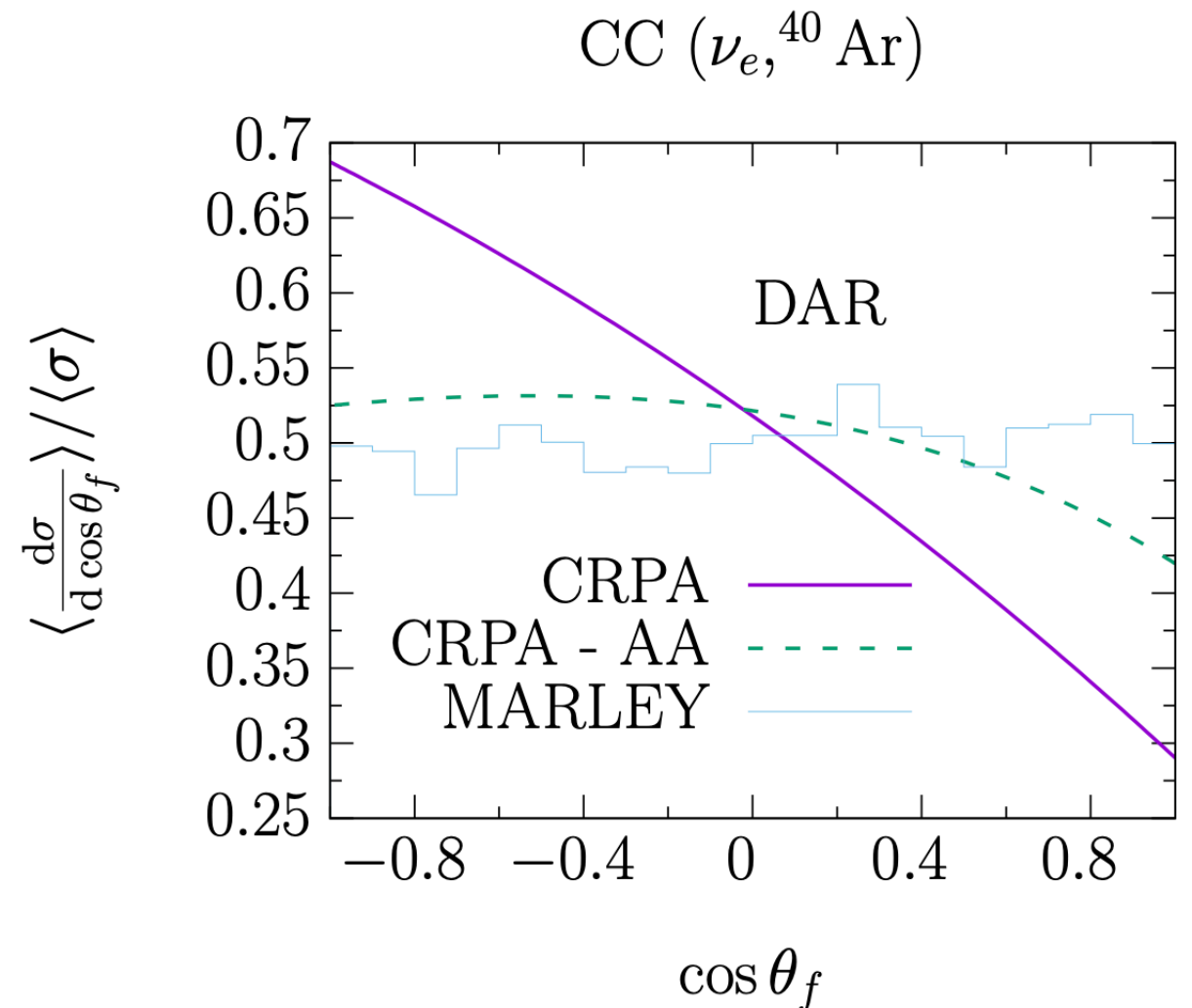
- [MARLEY](#) (Model of Argon Reaction Low Energy Yields) is a neutrino event generator specifically developed to simulate tens-of-MeV neutrino-nucleus interactions in liquid argon.

Steven Gardiner [arXiv:2010.02393 [nucl-th].

- An example of MARLEY ν_e CC event simulated in LArSoft, showing the trajectories and energy deposition points of the interaction products.



- CRPA implementation in MARLEY is currently on-going, in collaboration with Steven Gardiner.



- MARLEY predicts a nearly flat angular distribution (only allowed transitions, Fermi and Gamow Teller strengths).
- CRPA includes full expansion of nuclear matrix element (allowed as well as forbidden transition), predict more backwards strength.

Summary

- Experimental observation of CEvNS opened a new portal of searching weakly interacting new physics at low energies. SM expectation of CEvNS cross section have to be know at a precision that allows resolving degeneracies in the standard and non-standard physics observables.
- Future precise measurements of CEvNS cross section will enable precise determination of weak form factor at low momentum transfers and neutron density distributions of nuclei. These will provide vital input to modeling ground states of nuclei.
- CEvNS experiments at stopped-pion sources are powerful avenues to measure 10s of MeV inelastic CC and NC neutrino-nucleus cross sections. These measurements will play a vital role in enhancing future long baseline neutrino experiments' capability of detecting core-collapse supernovae neutrinos.
- We presented a consistent description of both coherent elastic and inelastic neutrino-nucleus scattering within a unified many-body nuclear theory approach. The model is currently being implemented in a dedicated low-energy neutrino event generator, MARLEY.